© 2009 The Chemical Society of Japan Bull. Chem. Soc. Jpn. Vol. 82, No. 5, 539–554 (2009)

Accounts

Angular Dipyridyl Ligands 2,5-Bis(4-pyridyl)-1,3,4-oxadiazole and Its 3-Pyridyl Analogue as Building Blocks for Coordination Architectures: Assemblies, Structural Diversity, and Properties

Miao Du[2] **and Xian-He Bu***[1]

[1]Department of Chemistry, Nankai University, Tianjin 300071, P. R. China

[2]College of Chemistry and Life Science, Tianjin Normal University, Tianjin 300387, P. R. China

Received September 9, 2008; E-mail: buxh@nankai.edu.cn

The rational design and construction of functional coordination architectures, which rely upon the docile assemblages of organic ligands with metal centers, have attracted continuing interest for many years. The selection of suitable organic ligands as building blocks is a key point for the construction of novel coordination architectures with desired structures and functions. This article will briefly review the coordination-driven assembly of angular dipyridyl-type building blocks involving the oxadiazole spacer, namely 2,5-bis(4-pyridyl)-1,3,4-oxadiazole and its 3-pyridyl-donor analog 2,5-bis(3-pyridyl)-1,3,4-oxadiazole, with transition-metal ions. Diversity of the established structural motifs thus far (only considering the coordination interaction) is outlined, illustrating the broad range of coordination frameworks from discrete molecular architectures to infinite extended one-, two-, and three-dimensional (1-D, 2-D, and 3-D) networks. The specific influencing factors such as anion, solvent, and metal-to-ligand ratio on structural assemblies and the interesting properties of anion exchange, magnetism, fluorescence, and guest inclusion of these crystalline solids will also be discussed.

1. Introduction

In the past decade, crystal engineering, as an exciting domain that attracts an increasing number of researchers, has become a nice paradigm for the development of a clear understanding of the relationship between individual molecules and functional materials as crystalline solids.[1a–1c] Although the term of crystal engineering was originated by Schmidt to refer to the topic of solid-state photochemistry of organic compounds,[1d] this theme is playing the role as an inherently interdisciplinary activity at present, and making a significant contribution to supramolecular chemistry, coordination chemistry, material science, molecular recognition, etc.[1e–1h]

Crystal engineering of coordination architectures provides a good strategy for achieving solid-state functional materials with potential applications in quite a few areas such as separation, catalysis, conductivity, gas absorption, chirality, luminescence, magnetism, and nonlinear optics.[2] Coordination crystalline architectures are primarily dependent on the foundation of coordination bonds for interconnecting the preselective building components, so as to meet the requirement of ligand function and metal binding tendency, as well as the energetic consideration of crystal packing for the overall supramolecular system.[3] Generally, the coordination geometries of metal centers appear in somewhat predictable patterns, ranging from linear, T- or Y-shaped, tetrahedral, square-planar, square-pyramidal, trigonal-bipyramidal, octahedral, trigonal-prismatic, and pentagonal-bipyramidal spheres, to their corresponding distorted forms, according to their intrinsic coordination preferences and oxidation states.[4]

On the other hand, the appropriate choice of well-designed organic bridging ligands as building blocks with adjustable information of connectivity or binding ability, such as the most common linear or angular bidentate spacers and more complicated multidentate connectors, has been proven to be a crucial element to fabricate fine-tuning functional crystalline architectures.[5] For instance, by using a rigid multitopic spacer ligand 3,6-di-2-pyridyl-1,2,4,5-tetrazine (DPTZ) as a suitable tectonic component, the quantitative preparation of a unique cyclic tetranuclear $\mathrm{Zn^{II}}$ molecular box can be achieved as spontaneously resolved chiral crystals (Scheme 1).[5d] In this context, multidentate bridging ligands containing two or more nitrogen, sulfur, and/or oxygen-donor groups with distinct binding ability to metal ions have been extensively explored. These organic building components are normally of neutral or anionic nature and can be mainly classified as several distinct types, such as the representative dipyridyl, polycarboxylate, pyridinecarboxylate, and thioether/thiolate, which have been reported to be effective for the construction of diverse discrete and/or extended coordination networks.[6] In this regard, in our

Published on the web May 13, 2009; doi:10.1246/bcsj.82.539

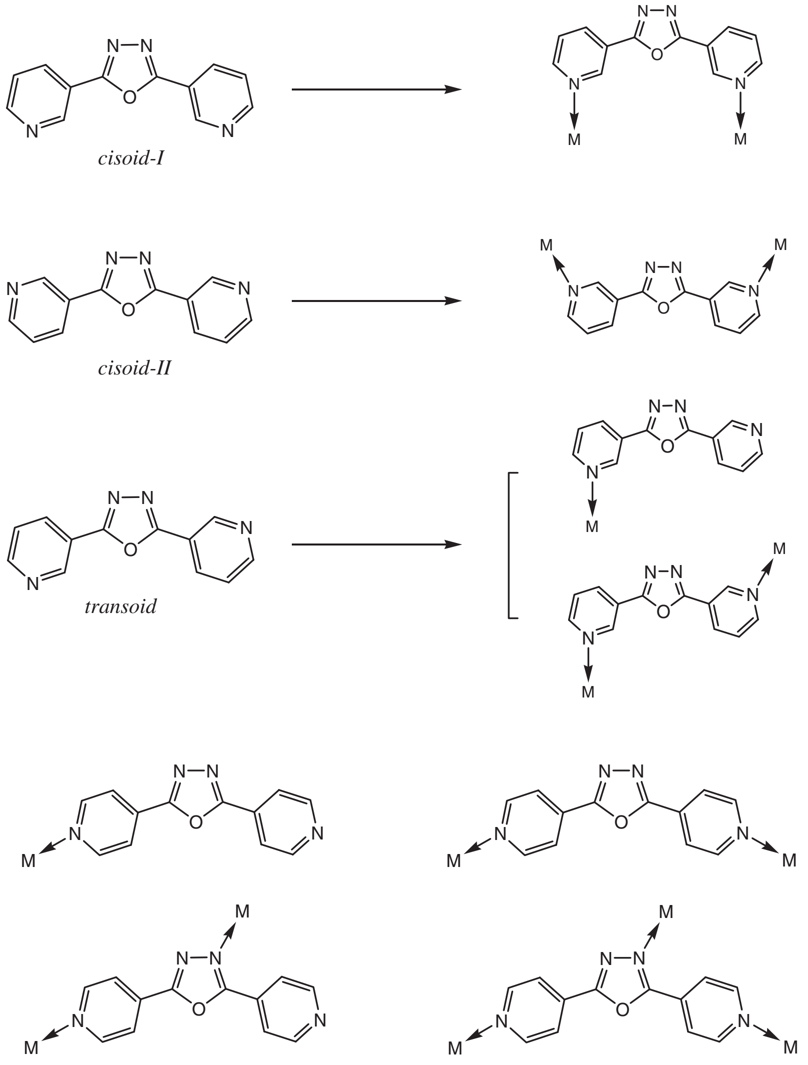

Chart 1.

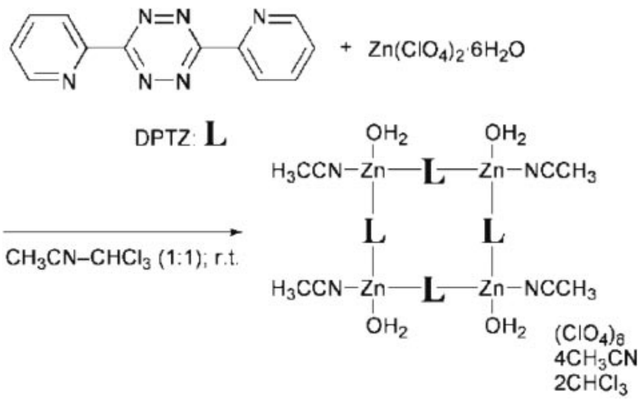

Scheme 1.

continuing efforts to explore the rational construction of functional coordination architectures, we have designed or selected several types of organic ligands as building blocks for multi-dimensional metallostructural assembly, such as bis(sulfinyl) compounds,[7] thioethers,[8] functional diazamesocycles,[9] polydentate N-donor systems,[10] ligands bearing bulky backbones,[11] as well as mixed ligands.[12]

As a series of excellent linkers between transition-metal ions for the propagation of coordination frameworks, the importance of exo-bidentate (or ambident) dipyridyl-type compounds, for instance, apparently the simplest 4,4-bipyridine and its analogs with modified spacers such as 1,2-bis(4-pyridyl)ethane, 1,3-bis(4-pyridyl)propane, and *trans*-bis(4-pyridyl)ethene, has been considerably noticed.[13] In this regard, a bent dipyridyl derivative 2,5-bis(4-pyridyl)-1,3,4-oxadiazole (4-bpo) and its 3-N-donor analog 2,5-bis(3-pyridyl)-1,3,4-oxadiazole (3-bpo) with variable conformations and coordination fashions (Chart 1) have also attracted intense attention recently. A variety of coordination architectures based on such angular dipyridyl building blocks and familiar metal ions (including Cu^{I}/Cu^{II}, Ag^{I}, Zn^{II}, Cd^{II}, Hg^{II}, Mn^{II}, Fe^{II}/Fe^{III}, Co^{II}, and Ni^{II}) have been documented, which will be comprehensively reviewed herein. A current Cambridge Structural Database (CSD) search (Version 5.29 of November 2007, plus one update, similarly hereinafter) indicates that the total numbers of coordination structures of 3-bpo and 4-bpo with these transition-metal ions are 23 and 45, respectively (see Figure 1 for details). Notably, other related crystalline species involving such two molecules, for example, multi-component complex-

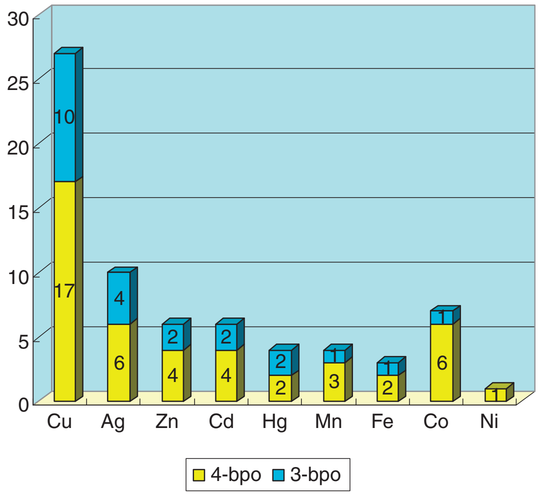

Figure 1. A schematic comparison of the amount of coordination species with ligands 4-bpo/3-bpo and various metal ions (on the basis of a current CSD search).

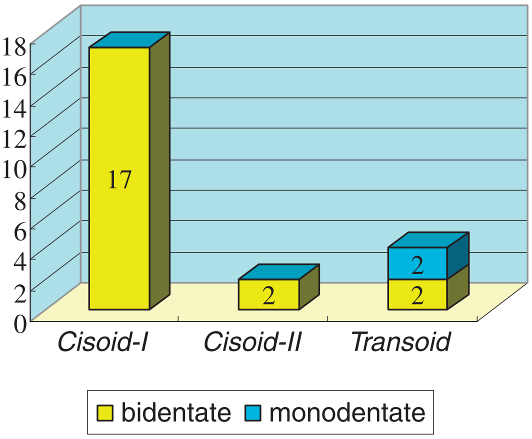

Figure 2. A schematic comparison of amount of coordination species involving 3-bpo with different conformations and binding modes (on the basis of a current CSD research).

Table 1. Statistics of Various Coordination Structures of 3-bpo with Different Transition-Metal Ions[a)]

	Discrete	1-D	2-D	3-D
Cu(10)	5	4	1	0
Ag(4)	2	2	0	0
Zn(2)	1	1	0	0
Cd(2)	0	0	2	0
Hg(2)	0	2	0	0
Mn(1)	1	0	0	0
Fe(1)	1	0	0	0
Co(1)	0	0	1	0

a) The number in parenthesis indicates the total amount of coordination structures with a given metal. The data are taken from a current CSD search (Version 5.29 of November 2007, plus one update, similarly hereinafter).

es,[14a] organometallic compounds,[14b,14c] and organic co-crystals or salts[14d,14e] have also been known, which however will be largely ignored in this account.

A plain strategy to achieve the rational modulation of the coordination behavior of rich heteroatom systems such as 1,3,4-oxadiazole here is to add rigid substituents carrying additional donor groups. This modification will create more available binding sites, improve the steric hindrance, and thus, make it feasible to promise more versatile and rich coordination chemistry. Representatively, the most simple and widely used substituent group for this goal is pyridyl, especially 3- and 4-pyridyl terminal for the bridging purpose. Additionally, there are some particular characteristics of the 3-bpo and 4-bpo building blocks as described below. (a) Both ligands can take various binding modes, such as monodentate (using one pyridyl nitrogen donor), bidentate bridging (using two pyridyl nitrogen donors or one pyridyl and one oxadiazole nitrogen donors), and tridentate bridging (using two pyridyl and one oxadiazole nitrogen donors) coordination to construct diverse coordination frameworks. (b) The structural geometries of the ligands are bent and variable. The dihedral angles between the oxadiazole group and two pyridyl rings as well as the angle between the center of oxadiazole and two terminal pyridyl nitrogen donors are adaptable to meet the coordination requirements upon metalation. (c) The aromatic groups in both ligands usually show a tendency to completely or partly participate in intermolecular π–π interactions, which may significantly affect the packing arrangements of coordination structures. (d) Especially for 3-bpo, theoretically, it has the potential tendency to adopt three typical conformations to self-adjust the coordination assembles, which will give rise to distinct structural motifs under appropriate conditions (Chart 1).

According to the result of a CSD analysis (Figure 2), the occurrence frequencies of cisoid-I, cisoid-II, and transoid conformations of 3-bpo are 17, 2, and 4, respectively, among total 23 3-bpo involved coordination complexes. Notably, all cisoid-I- and cisoid-II-styled 3-bpo ligands adopt the bidentate bridging fashion via the pyridyl nitrogen, facilitating the formation of dinuclear, 1-D, and 2-D coordination motifs. Only two out of four coordination structures with transoid-styled 3-bpo are found to show a monodentate mode of the ligand in the monomeric complex unit, among all 23 known examples (9% probability). Based on the complexity of its binding mode and conformation, the combination of 3-bpo with different transition-metal salts affords various coordination structures, from discrete molecules, to 1-D and 2-D networks, as depicted in Table 1 and Scheme 2. From the data in Table 1, it is indicated that the most probable resultant crystalline structures are discrete and 1-D motifs (19 of total 23 complexes, 83% probability), and singularly, no 3-D coordination framework is known so far, no matter what the metal ion and anionic co-ligand.

Considering the coordination patterns of 4-bpo in the structure-determined complexes, the database covers 46 related results, in which the numbers of monodentate, bidentate, and tridentate 4-bpo ligands are 17, 28, and 4, respectively, for the angular coordination essence (Figure 3). It is noteworthy that the central oxadiazole ring does not serve as a silent spectator anymore, and participates in accomplishing the coordination complexes, providing the 4-bpo ligand as a tridentate linker. As

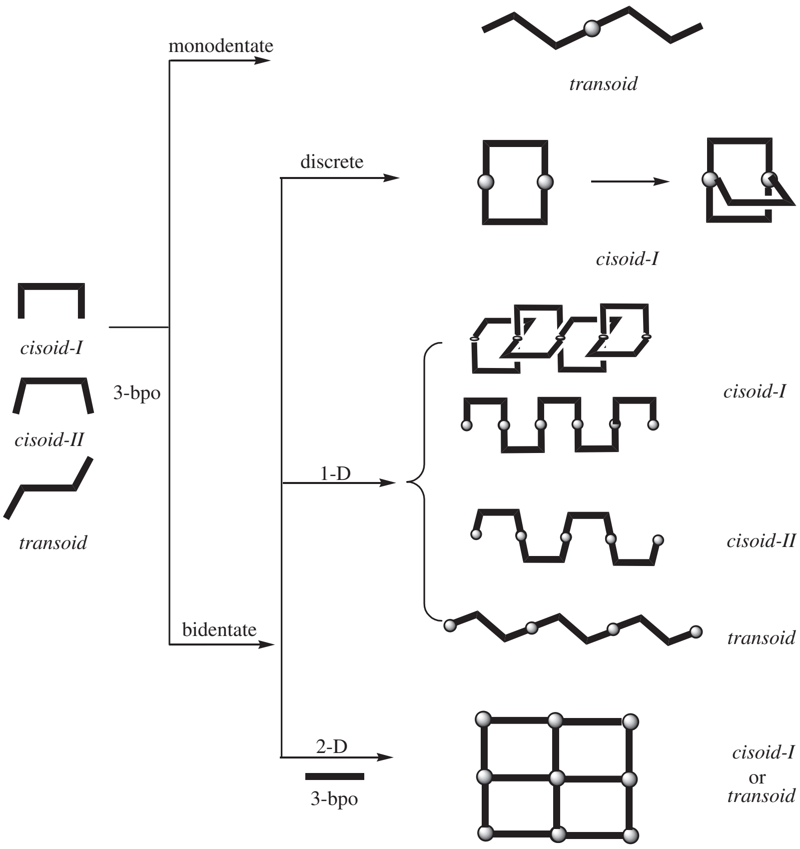

Scheme 2.

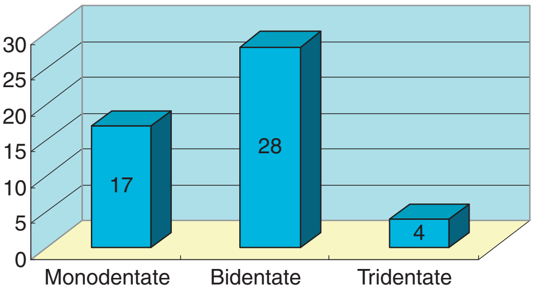

Figure 3. A schematic comparison of amount of coordination species involving 4-bpo with different binding modes (on the basis of a current CSD search).

Table 2. Statistics of Various Coordination Structures of 4-bpo with Different Transition-Metal Ions[a)]

	Discrete	1-D	2-D	3-D
Cu(17)	4	4	2	7
Ag(6)	0	4	2	0
Zn(4)	1	3	0	0
Cd(4)	1	1	1	1
Hg(2)	0	1	1	0
Mn(3)	3	0	0	0
Fe(2)	2	0	0	0
Co(6)	3	2	1	0
Ni(1)	0	0	1	0

a) The number in parenthesis indicates the total amount of coordination structures with a given metal. The data are taken from a current CSD search.

listed in Table 2, the 4-bpo ligand displays affinity for copper and silver centers for the specific complexes derived from these two metals counting over 50% of total, and this is also the case for the 3-bpo ligand. A large amount of coordination architectures derived from 4-bpo with the given metal ions have been synthesized, which exhibit multifarious structural types ranging from discrete molecules, 1-D zigzag or comb-like chains, 2-D grid-like layers, to 3-D reticular frameworks with open or interpenetrated prototype, as shown in Scheme 3.

With regard to such unusual dipyridyl building blocks 3-bpo and 4-bpo with bent backbones, the different relative orientations of the pyridyl nitrogen donors result in the dissimilar binding nature (especially the flexible conformation of 3-bpo that is adopted to cater to coordination prerequisites under appropriate conditions), which in turn lead to the formation of various coordination architectures. Into the bargain, the ultimate structures have also been shown to depend on several factors such as the coordination tendency of metal ion, guest molecule, ligand-to-metal ratio used in the reactive process, counter anion, and even solvent, which will also be discussed in this account. The objective of this article focuses upon a comprehensive overview of the availability and general coordination chemistry of the angular dipyridyl ligands 3-bpo and 4-bpo, which may provide a useful guide for the further design and preparation of the related functional coordination systems in the future. Beyond this, some interesting properties for the known crystalline solids such as anion exchange,

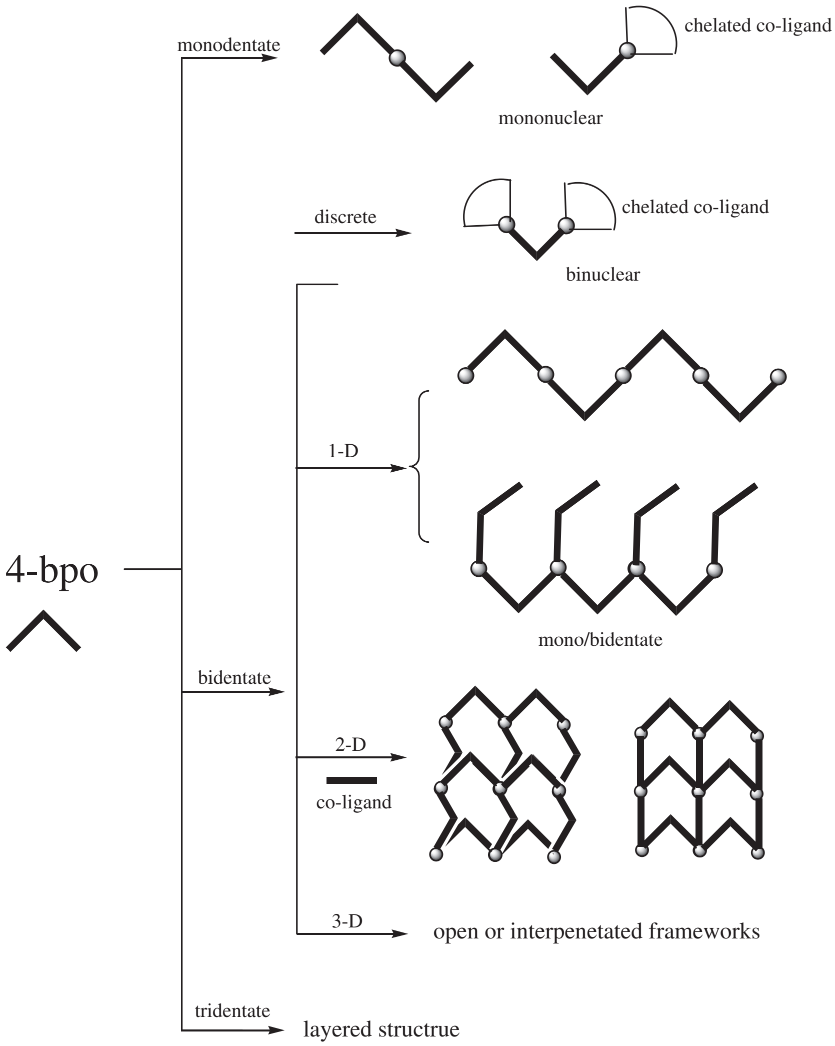

Scheme 3.

luminescence, magnetism, and guest inclusion will also be discussed.

2. Coordination Chemistry of the Ligands

2.1 Monodentate Coordination. The presence of monodentate bpo-type ligands usually decreases the extended tendency of the resultant complexes and thus affords discrete coordination motifs. Notably, under these circumstances, the 3-bpo ligand always adopts the transoid conformation to avoid the steric hindrance and the uncoordinated pyridyl groups in both 3-bpo and 4-bpo are facilely involved in hydrogen-bonding and/or aromatic stacking interactions to construct extended supramolecular networks.

For instance, in the molecular structures of the isostructural Mn^{II} and Fe^{II} mononuclear complexes $[M(3\text{-bpo})_2(H_2O)_2(NCS)_2]$,[15] each metal ion is located at an inversion center and six-coordinated to two nitrogen atoms of the monodentate thiocyanate ions, two water molecules, and two pyridyl nitrogen donors of the 3-bpo ligands. The unidentate 3-bpo molecules adopt the unusual transoid conformation with respect to the terminal pyridyl groups, so as to favor the hydrogen bonds between the uncoordinated 3-pyridyl nitrogen atoms and the aqua ligands to afford a layered supramolecular network (Figure 4). In addition, aromatic interactions between the pyridyl rings are also found to stabilize the overall crystalline lattice.

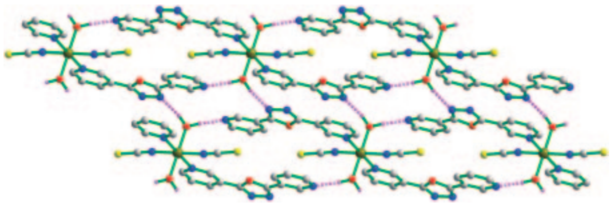

Figure 4. 2-D hydrogen-bonded (broken lines in purple) layer in the crystal structures of $[M(3\text{-bpo})_2(H_2O)_2(NCS)_2]$ ($M = Mn^{II}$ and Fe^{II}).

Comparatively, the 4-bpo ligand presents a tendency to construct mononuclear coordination motifs (a total of thirteen examples are known and seven of them are based on metal perchlorate). For example, assemblies of 4-bpo with a series of metal perchlorates ($M = Mn^{II}$, Fe^{II}, Co^{II}, Zn^{II}, and Fe^{III}) in $CH_3OH/CH_3CN/H_2O$ mixed medium afford five new supramolecular complexes with the general formula $[M(4\text{-bpo})_2(H_2O)_4](anion)\cdot 2(4\text{-bpo})\cdot(solvent)$.[16a] In these similar cationic

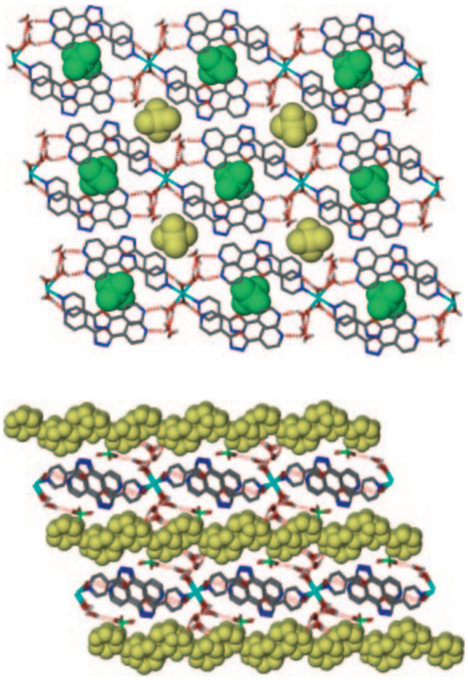

Figure 5. 3-D supramolecular lattices of $[M(4\text{-bpo})_2(H_2O)_4](\text{anion})\cdot 2(4\text{-bpo})\cdot(\text{solvent})$ (top) $M = Mn^{II}$, Zn^{II}, and Fe^{III} and (bottom) $M = Fe^{II}$ and Co^{II}.

monomeric complex units, each metal ion is located at the crystallographic inversion center and six-coordinated to four aqua ligands and two monodentate 4-bpo ligands. Interestingly, although similar molecular structures and compositions are found for these mononuclear complexes, they display two types of supramolecular lattices, as shown in Figure 5. The Mn^{II}, Zn^{II}, and Fe^{III} coordination species similarly crystallize in space group $P2/n$ or $P2/c$, in which the cationic complex units, free 4-bpo molecules, and lattice water guests are interlinked to form 2-D layered supramolecular frameworks with the aid of hydrogen bonding, and the perchlorate anions are located within and between (also methanol in the Fe^{III} complex) these 2-D arrays (Figure 5 top). On the other hand, the isostructural Fe^{II} and Co^{II} complexes crystallize in space group $P\bar{1}$, in which two types of layered arrays respectively constituted by the cationic complex units and uncoordinated 4-bpo components are found, and the perchlorate anions and lattice water molecules are located between such alternate layers (Figure 5 bottom). As a result, a complicated 3-D network is formed via the linkage of these subunits by intermolecular hydrogen bonds. However, when Mn^{II} perchlorate is used to react with 4-bpo in CH_3CN/H_2O mixed solvents, another monomeric complex $[Mn(4\text{-bpo})_2(CH_3CN)_2(H_2O)_2](ClO_4)_2\cdot 2CH_3CN$ is obtained.[16b] In this structure, the Mn^{II} ion is also located at the crystallographic inversion center to furnish a slightly distorted octahedral coordination geometry, leaving the uncoordinated pyridyl group of 4-bpo available for secondary interactions. Another very similar structural illustration of $[Cu(4\text{-bpo})_2(ClO_4)(H_2O)_3](ClO_4)\cdot H_2O$ is generated from the reaction of copper(II) perchlorate with 4-bpo in CH_3OH/H_2O medium, except that one ClO_4^- is bound to the Cu^{II} center instead of solvent.[16c]

When thiocyanate ion is introduced into the assembled system, a series of isostructural mononuclear complexes with the formula $[M(4\text{-bpo})_2(H_2O)_2(NCS)_2]$ ($M = Mn^{II}$, Co^{II}, Fe^{II}, and Cd^{II}) are obtained.[17a,17b] In these structures, the monomeric complex molecules are also extended to 3-D supramolecular networks via hydrogen bonding and aromatic stacking. While in the structure of complex $[Cu(4\text{-bpo})_2(H_2O)(OAc)_2]$, the Cu^{II} center is penta-coordinated (CuN_2O_3) to two pyridyl nitrogen atoms from the unidentate 4-bpo molecules, as well as three oxygen donors from the terminal acetate anions and one aqua ligand.[5a] Furthermore, the combination of 4-bpo, cobalt(II) acetate, and organic dianion pyridine-2,6-dicarboxylicate (pydc) leads to the formation of an unusual mononuclear complex $[Co(4\text{-bpo})(H_2O)_2(\text{pydc})]\cdot H_2O$, in which the distorted octahedral sphere of Co^{II} is completed by the tridentate chelated pydc organic anion, two water molecules, and one protrudent 4-bpo ligand as pendant.[17c] Attractively, such unsymmetrical monomeric coordination motifs are further interconnected via hydrogen bonding and aromatic stacking to establish a 3-D microporous framework with the guest water molecules being included in the available 1-D columned channels. Distinguishingly, the reaction of cadmium(II) iodide with 4-bpo affords a 1-D chain array $[Cd(4\text{-bpo})_2(\mu\text{-}I)_2]_n$,[6d] in which the cadmium ions are connected by paired iodide bridges to generate infinite $[CdI_2]_n$ chains while the 4-bpo molecules serve as the unidentate terminals.

2.2 Bidentate Coordination. Normally and essentially, both ligands 3-bpo and 4-bpo are considered to be exo-bidentate building blocks and undisputedly play the bridging role by using the terminal pyridyl groups. Nevertheless, another distinct category may also be observed, which involves one pyridyl and one oxadiazole nitrogen donors (Chart 1). In this connection, various coordination architectures can be assembled from both ligands with bidentate coordination modes.

2.2.1 Discrete Binuclear Complexes (0-D): Obviously, the 3-bpo bridging ligand with cisoid-I conformation will facilitate the formation of cyclic binuclear complexes, and up to now, eight such coordination motifs with the metal ions of Cu^{I}, Cu^{II}, Ag^{I}, and Zn^{II} have been reported. Reactions of copper(II) perchlorate, nitrate, or tetrafluoroborate with 3-bpo under general conditions afford three similar bimetallic macrocyclic species $[Cu_2(3\text{-bpo})_2(H_2O)_6](ClO_4)_4\cdot 4H_2O$, $[\{Cu(NO_3)_2(3\text{-bpo})\}_2]\cdot 2CH_3CN$, and $[Cu_2(3\text{-bpo})_2(H_2O)_6](BF_4)_4\cdot 3H_2O$.[18a,18b] In each case, two Cu^{II} centers with square-pyramidal geometries are connected by a pair of *cisoid-I*-3-bpo linkers to result in a discrete $[M_2(3\text{-bpo})_2]$ metallacycle, which represents the smallest closed cyclic structure with a 1:1 metal-to-ligand ratio, as illustrated in Figure 6 top. The dimensions of such rectangular metallacycles are ca. 7.9×7.3, 7.6×7.4, and 7.9×7.3 Å^2, with intra-ring Cu···Cu distances of 7.985, 7.376, and 7.962 Å. Similar association of the Cu^{II}-based metallacyclic motif is also found in the structure of $[Cu(\text{Hfum})_2(3\text{-bpo})(H_2O)]_2\cdot 2(3\text{-bpo})\cdot 6H_2O$ ($H_2\text{fum}$ = fumaric acid), in which the organic anion is unidentate coordinated. Unexpectedly, the uncoordinated 3-bpo molecules in this case have the rare cisoid-II conformation and are included in the final 3-D crystalline lattice as guest templates.[18c]

We have also designed and synthesized a flexible 3,3′-dipyridyl ligand with a diazamesocycle as spacer, namely *N,N*′-

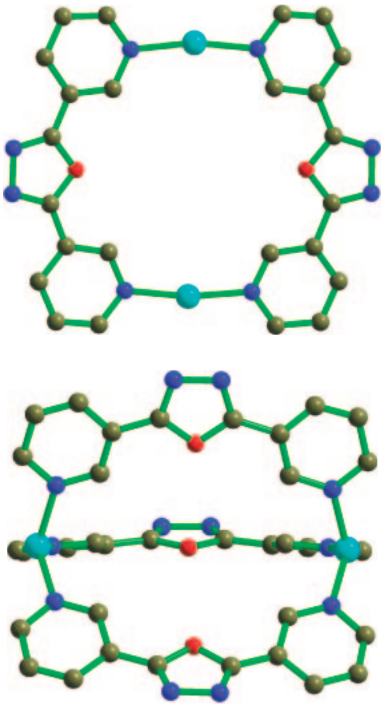

Figure 6. Two types of binuclear metallamacrocycles in (top) $[Cu^{II}_2(3\text{-bpo})_2(H_2O)_6]^{4+}$ and (bottom) $[Cu^{I}_2(3\text{-bpo})_3(CH_3CN)_2]^{2+}$.

bis(pyrid-3-ylmethyl)-1,5-diazacyclooctane (**L**). Self-assembly of copper(II) perchlorate with **L**$\cdot$4HCl$\cdot$4H_2O affords a chain coordination polymer $\{[CuCl(\mu\text{-}H_2\mathbf{L})(\mathbf{L})](ClO_4)_3\}_n$ instead of the bimetallic macrocyclic motif, in which the ligands display two different coordination modes (cis chelated and trans bridged) with the Cu^{II} ions.[19a] Interestingly, when its 4-*N*-pyridyl analogous **L′** is used to react with copper(II) chloride, a unique paramagnetic Cu^{II} metallamacrocycle $[CuCl_2(H\mathbf{L'})]_2(ClO_4)_2$ is obtained due to the considerable ligand flexibility, in which the ferromagnetic exchange interaction is found between the Cu^{II} centers.[19b]

Notably, when copper(I) tetrafluoroborate is used to assemble with 3-bpo, a novel cage-shape species $[Cu_2(3\text{-bpo})_3(CH_3CN)_2](ClO_4)_2\cdot H_2O$ with trigonal-prismatic geometry is obtained, in which the two adjacent Cu^{I} centers that adopt distorted tetrahedral geometries are linked by three 3-bpo ligands with cisoid-I conformation (Figure 6 bottom).[18b] It is interesting that the resulting complex cation hosts a guest water molecule within the inner cavity with a Cu···Cu distance of ca. 5.9 Å, which further stabilizes this coordination polyhedron. Thus, we can undoubtedly conclude that the nature of metal center is of key importance in the structural assembly of distinct $[M_2(3\text{-bpo})_2]$-ring or $[M_2(3\text{-bpo})_3]$-cage motifs due to their different coordination tendencies and geometries.

As for other related dinuclear species, complex $[Zn(3\text{-bpo})(H_2O)_3(NO_3)]_2(NO_3)_2$[20a] displays a planar macrocyclic motif with dimension of ca. 7.9 × 7.3 $Å^2$, in which the two octahedral Zn^{II} centers are similarly linked by the *cisoid-I*-3-bpo ligands. In addition, two centrosymmetric binuclear macrocyclic complexes with the general formula $[Ag_2(3\text{-bpo})_2](\text{anion})_2$ (anion = SbF_6^- and $CF_3SO_3^-$) have also been isolated from 3-bpo and the corresponding silver(I) salt.[20b,20c]

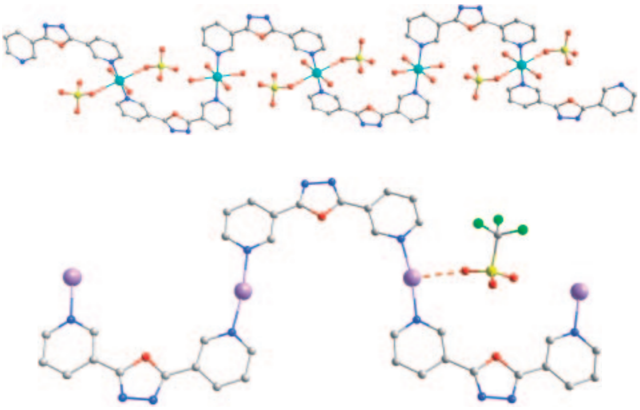

Figure 7. 1-D coordination chain motifs in (top) $\{[Cu_2(3\text{-bpo})_2(H_2O)_6(SO_4)_2]\cdot 6H_2O\}_n$ and (bottom) $\{[Ag(3\text{-bpo})]CF_3SO_3\}_n$ with *cisoid-I*-3-bpo ligands.

With regard to the metallosupramolecular assembly based on 4-bpo, it can be easily deduced that the formation of above-mentioned bimetallic macrocyclic structural motifs will be unfavorable due to the change of pyridyl nitrogen terminals and thus the coordination orientation (more divergent) of ligand. Instead, a dissimilar dinuclear Cu^{II} complex $[Cu_2(4\text{-bpo})(H_2O)_3(pydc)_2]\cdot 2.75H_2O$ is obtained by the reaction of copper(II) salt with the combination of H_2pydc and 4-bpo ligands under either ambient or hydrothermal conditions. In this instance, each neutral dimeric coordination unit consists of two Cu^{II} centers chelated to a pair of pydc terminals and bridged by one 4-bpo ligand as spacer, which display different coordination spheres of distorted square pyramid and octahedron, respectively.[17c]

2.2.2 1-D Coordination Polymer: The majority of coordination polymers with 3-bpo and 4-bpo ligands are 1-D arrays. This observation could be ascribed to the nature of metal ions—these nodes have limited coordination numbers (no more than six) and the effective linkage for network assembly is usually prevented by the coordination competition of the terminal anions and/or solvents. As a result, the known 1-D polymerized products can be classified into two categories based on geometries of the coordination patterns, from the popular zigzag (metal/ligand molar ration of 1/1) to unusual double sinusoidal, comb-like, and binuclear paddle-wheel based chains (metal/ligand molar ratio of 1/2).

2.2.2.1 Zigzag Chain Motif; To date, all the theoretically possible conformations of the 3-bpo ligand, namely cisoid-I, cisoid-II, and transoid, have shown the tendency to produce zigzag coordination polymers with familiar metal ions such as Cu^{II}, Ag^{I}, Zn^{II}, and Hg^{II}. In the neutral 1-D infinite alternate chain motif of complex $\{[Cu_2(3\text{-bpo})_2(H_2O)_6(SO_4)_2]\cdot 6H_2O\}_n$, two independent octahedral Cu^{II} centers with different coordination environments are bridged by the 3-bpo spacers with cisoid-I conformation (Figure 7 top).[18a] Other than the bimetallic macrocyclic complexes stated above,[20b,20c] reactions of AgX (X = SbF_6^- and $CF_3SO_3^-$) with 3-bpo under appropriate conditions may also produce two similar cationic 1-D coordination chains $\{[Ag(3\text{-bpo})]^+\}_n$ bridged by the *cisoid-I*-3-bpo ligands,[20b,21a] in which the large counter anions are located within the grooves of the 1-D arrays (Figure 7 bottom).

Moreover, crystallization of 3-bpo with copper(II) hexafluoroacetylacetonate (hfacac) in CH_3OH/CH_2Cl_2 solution yields the infinite 1-D polymeric compound $[Cu(hfacac)_2(3\text{-bpo})]_n$, which exhibits a single sinusoidal-chain motif with the hfacac anions and unique cisoid-II conformational 3-bpo ligands playing the chelating and bridging roles, respectively.[21b]

When d^{10} metal halides are applied in the self-assembled systems, 1-D wave-like polymeric coordination polymers can also be obtained. In the crystal structure of complex $[Zn(3\text{-bpo})Cl_2]_n$ prepared from $ZnCl_2$ and equimolar 3-bpo, the tetrahedral Zn^{II} coordination sphere is built up by two chloride ligands and two pyridyl nitrogen donors of the bridging 3-bpo ligands with unusual transoid conformation, giving rise to a 1-D zigzag coordination chain with the ligand/metal composition of 1/1.[22a] In the case of 1-D coordination arrays of $[Hg(3\text{-bpo})X_2]_n$ ($X = Br^-$ and I^-), each Hg^{II} center is also surrounded by two halide counter ions and a pair of 3-bpo ligands but with the cisoid-I conformation to complete a distorted tetrahedral coordination environment.[22b,22c]

Comparatively, the monotonous 4-bpo bridging ligands prefer to interlink metal ions such as Co^{II}, Zn^{II}, Ag^{I}, and Hg^{II}, resulting in similar 1-D crooked chains. In this context, reactions of the ligand 4-bpo with $CoSO_4$ and $Co(NO_3)_2$ lead to the formation of two extended polymeric chains, namely $\{[Co(4\text{-bpo})(H_2O)_3(SO_4)]\cdot 2CH_3OH\}_n$[6d] and $\{[Co(4\text{-bpo})(H_2O)_2(NO_3)_2]\cdot 3H_2O\}_n$,[16a] in which the Co^{II} centers are also coordinated by the anions and aqua molecules, besides the 4-bpo linkers. As for the ZnX_2 species ($X = Cl^-$,[22b] NO_3^-,[20a] and ClO_4^-[20a]), the polymerization with 4-bpo coherently demonstrates the 1-D propagating nature, regardless of the different Zn^{II} coordination spheres in these structures (tetrahedron for chloride and octahedron for nitrate and perchlorate). Similarly, in the coordination polymeric chains of $\{[Ag(4\text{-bpo})]^+\}_n$ with NO_3^-,[22d] BF_4^-,[16b] and ClO_4^-[22e] as counter anions, no significant divergence of the coordination frameworks is found, arising from their reliable accommodation of different anions. Furthermore, the combination of 4-bpo and HgI_2 in the mixed solvents of CH_2Cl_2/CH_3CN affords a 1-D coordination polymer $\{[HgI_2(4\text{-bpo})]\cdot CH_3CN\}_n$[22b] with a zigzag chain motif, in which the uncoordinated CH_3CN molecules are located between the parallel coordination chains with none significant interchain interactions.

2.2.2.2 Double Sinusoidal Array; Only one example for this structural type is found by crystallization of 3-bpo with $Cu(ClO_4)_2$ in a methanol/methylene chloride mixed-solvent system at room temperature, which affords a 1-D polymeric complex $\{[Cu(3\text{-bpo})_2(ClO_4)]ClO_4\}_n$ with the metal/ligand ratio of 1/2.[21b] In this structure, the metal center displays a square-pyramidal environment, consisting of four equatorial pyridyl N-donors from four *cisoid-I*-3-bpo ligands and one axial interaction with one oxygen of the ClO_4^- counter ion. As a result, the Cu^{II} centers are doubly connected to each other by two sets of curved 3-bpo ligands to give a novel double-sinusoidal chain motif extended along the [010] direction (Figure 8), in which one set of 3-bpo lies along (110) while the other along (011).

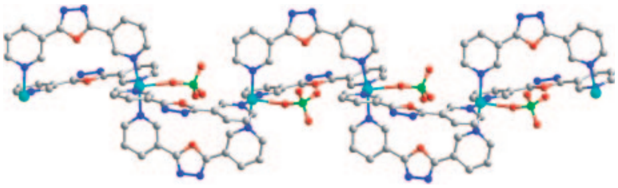

Figure 8. 1-D double sinusoidal chain coordination motif in $\{[Cu(3\text{-bpo})_2(ClO_4)]ClO_4\}_n$ with cisoid-I conformational 3-bpo linkers.

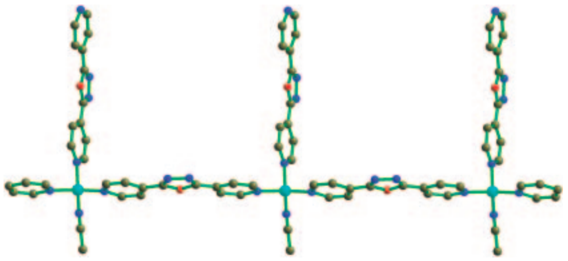

Figure 9. 1-D comb-like chain motif assembled from 4-bpo and Cu^I.

2.2.2.3 Comb-Like 1-D Polymer; In contrast, the analogous reactions of 4-bpo with univalent copper salts of $[Cu(CH_3CN)_4]ClO_4$[22f] and $[Cu(CH_3CN)_4]BF_4$[18b] in CH_3CN/CH_3OH generate two orange crystalline products formulated as $\{[Cu(4\text{-bpo})_2(CH_3CN)]ClO_4\cdot CH_3CN\cdot 1.5H_2O\}_n$ and $\{[Cu(4\text{-bpo})_2(CH_3CN)]BF_4\cdot 1.5H_2O\}_n$, respectively, with the metal-to-ligand ratio of 1:2. In both structures, each Cu^I center takes a tetrahedral sphere, coordinating to four nitrogen atoms from three 4-bpo ligands plus one acetonitrile. Remarkably, the 4-bpo ligands here display two types of coordination modes with the Cu^I ions, in which the bidentate bridges extend the Cu^I centers to form a 1-D chain (the adjacent Cu···Cu distances for ClO_4 and BF_4 species being 13.490 and 13.476 Å, respectively) and the monodentate terminals locate on one side of the chain, leading to the formation of a novel comb-like motif, as illustrated in Figure 9. Such a different coordination pattern from those of the Cu^{II} species may arise from the distinct coordination tendency and geometry of the Cu^I center. Although both Cu^I coordination polymers show similar 1-D structures, further analysis of the crystal packing reveals some interesting structural difference. In the case of copper(I) tetrafluoroborate complex of 4-bpo, the monodentate 4-bpo ligands from different 1-D arrays are arranged alternately along [010], whereas those in the copper(I) perchlorate complex are overlapped along [010] with significant aromatic stacking interactions. As a consequence, the latter stacking mode leads to the formation of larger channel volumes (662 Å^3, 37.2% of the unit-cell volume) than those in the former complex (320 Å^3, 21.0% of the unit-cell volume), in which the counter anions and solvent guests are included.

2.2.2.4 Coordination Chain with Dinuclear Paddle-Wheel Nodes; Under suitable conditions, the acetate ions can be used as the anionic building blocks and readily exhibit syn,syn bridging to constitute a reliable $[Cu_2(\mu\text{-OAc})_4]$ binuclear unit. For instance, assembly of 3-bpo with $Cu(OAc)_2$ in CH_3CN/CH_3OH medium furnishes a 1-D complex $\{[Cu_2(3\text{-bpo})(\mu\text{-OAc})_4]\}_n$,[18a] in which the $[Cu_2(\mu\text{-OAc})_4]$ dinuclear entities (Figure 10 top) are further extended by the 3-bpo ligands with rare cisoid-II conformation to facilitate a 1-D coordination array (Figure 10 bottom). Notably, elaborate

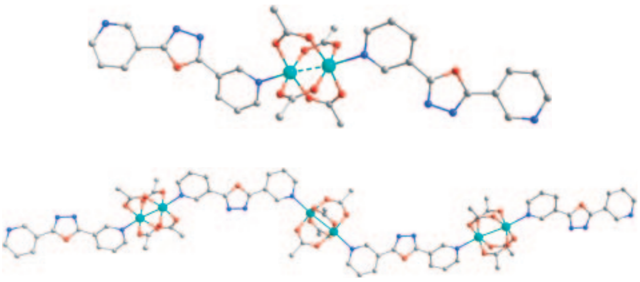

Figure 10. (top) Binuclear paddle-wheel subunit and (bottom) 1-D coordination chain motif in complex $\{[Cu_2(3\text{-bpo})(\mu\text{-OAc})_4]\}_n$.

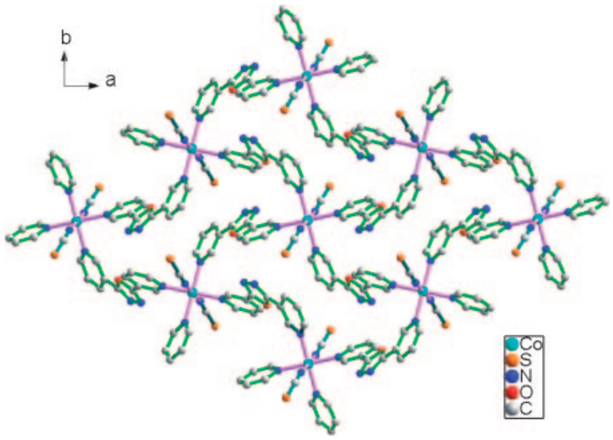

Figure 11. Layered framework of $[Co(3\text{-bpo})_2(NCS)_2]_n$ based on *transoid*-3-bpo linkers.

treatments of $Cu(OAc)_2$ with 4-bpo under different reaction conditions may lead to the formation of a series of comparable coordination polymers that are generally formulated as $\{[Cu_2(4\text{-bpo})(\mu\text{-OAc})_4]\cdot\text{solvent}\}_n$. In practice, if the coordination-driven assembly is performed in CH_3OH medium with the metal-to-ligand ratio of 1/1 or 2/1, the corresponding complex $\{[Cu_2(4\text{-bpo})(\mu\text{-OAc})_4]\cdot 2CH_3OH\}_n$[6d] or $\{[Cu_2(4\text{-bpo})(\mu\text{-OAc})_4]\cdot 3H_2O\}_n$[23a] is produced, whereas under the circumstance of $CH_3CN/CHCl_3$, another similar solvate $[Cu_2(4\text{-bpo})(\mu\text{-OAc})_4]\cdot CHCl_3\}_n$ can also be isolated.[23b] In these three isostructural complexes, 1-D coordination chains based on the paddle-wheel type $[Cu_2(\mu\text{-OAc})_4]$ dinuclear nodes and the 4-bpo linkers are formed with the inclusion of different lattice solvent molecules.

2.2.3 Layered Coordination Network: Up to now, four coordination polymers with 2-D layered coordination frameworks have been reported based on the 3-bpo linkers and/or other bridging co-ligands. In the crystal structure of $[Cd(3\text{-bpo})(H_2O)(\mu\text{-NO}_3)_2]_n$,[22b] two types of Cd^{II} centers with different seven- and six-coordinated environments are interconnected by the 3-bpo ligands with cisoid-I conformation and bridging nitrate anions to generate a layered network. As for complexes $\{[Cu(3\text{-bpo})(H_2O)_2(\mu\text{-suc})]\cdot 1.75H_2O\}_n$ and $\{[Cd_2(3\text{-bpo})(H_2O)_2(\mu\text{-suc})_2]\cdot 6.75H_2O\}_n$ (H_2suc = succinic acid),[18c] similar 2-D metal–organic coordination networks are observed in which the metal centers are linked by bidentate suc^{2-} and 3-bpo ligands with cisoid-I conformation. Notably, these 2-D layers display the interdigitated packing mode with the presence of interlayer π–π stacking interactions between the adjacent 3-bpo segments, which may reinforce the 3-D supramolecular lattices. Remarkably, the variable conformation of 3-bpo also leads to a completely different 2-D coordination polymer $[Co(3\text{-bpo})_2(NCS)_2]_n$,[6a] in which the octahedral Co^{II} centers are interconnected by only the *transoid*-3-bpo bridges to result in a 2-D undulating (4,4) layer with unidentate thiocyanate terminals (Figure 11). These layers are also stacked in the interdigitated fashion to decrease the steric hindrance of the final 3-D crystalline lattice.

Constitutionally, the bridging bidentate coordination characteristic of 4-bpo makes a sound explanation to join the metal centers to 1-D infinite transmission, and with the involvement of further linkages from additional assistant connectors such as anions, 2-D layered architectures can be easily achieved. The first structural paradigm on this issue occurs in the cobalt(II) sulfate complex $\{[Co(4\text{-bpo})(CH_3OH)_2(SO_4)]\cdot CH_3OH\cdot 3.5H_2O\}_n$ crystallized from methanol solvent.[16c] In this case, the Co^{II} centers are interlinked by 4-bpo ligands into zigzag chains, which are further extended by the bridged sulfate anionic components to form a 2-D coordination architecture. It seems that the replacement of sulfate with perchlorate in the assembled system will obscure the bridging fashion of anion due to its weaker coordination ablility.[16a] Even though a distinct 2-D coordination polymer $\{[Cu(4\text{-bpo})_2(H_2O)_2](ClO_4)_2\cdot 2(4\text{-bpo})_2\cdot CH_3OH\cdot H_2O\}_n$ with layered network bridged by 4-bpo spacers is obtained via subtly changing the assembled conditions, and the 3-D lattice with a parallel stacking of the 2-D layers possesses large rhombus-grid cavities for the inclusion of uncoordinated 4-bpo ligands, perchlorate counter anions, and lattice solvent molecules of methanol and water.[16c] In its Cd^{II} analog $\{[Cd(4\text{-bpo})_2(CH_3CN)_2](ClO_4)_2\cdot 2CH_3CN\}_n$,[22b] a similar 2-D layered pattern with bridging the octahedral Cu^{II} ions via 4-bpo spacers is found. However, these 2-D undulating layers are offset in the crystalline lattice to effectively reduce the volume of the cavities. Nevertheless, there exist available square cavities with the dimension of ca. $6 \times 7\,Å^2$, in which the guest CH_3CN molecules and perchlorate anions are located. The organic dicarboxylate anions such as the flexible building component 1,4-cyclohexanedicarboxylate ($chdc^{2-}$) and the above-mentioned suc^{2-} have also been employed as bridging bidentate ligands to furnish 2-D coordination polymers together with the 4-bpo spacers. The combination of copper(II) acetate and mixed ligands of H_2chdc/4-bpo gives rise to the formation of $\{[Cu(4\text{-bpo})(chdc)(H_2O)]\cdot 0.5H_2O\}_n$,[24a] which has a 2-D neutral coordination network extended by the bridging e,e-trans conformational $chdc^{2-}$ anions and 4-bpo ligands with the dimension of $13.6 \times 11.3\,Å^2$ for each repeating unit. These 2-D layers adopt the parallel stacking mode, creating large quadrate microporous cavities with the volume of $2805\,Å^3$. The layered structure of a comparable complex[18c] $\{[Ni(4\text{-bpo})(H_2O)_2(suc)]\cdot 5H_2O\}_n$ is shown in Figure 12. However, in this case, the 2-D arrays with the dimension of $13.8 \times 8.9\,Å^2$ for the rectangle grid unit are offset, which thus allows the significantly smaller void volume of only $190.0\,Å^3$.

In all 2-D coordination motifs stated above, the 4-bpo component is demonstrated as a typical exo-bidentate linker by

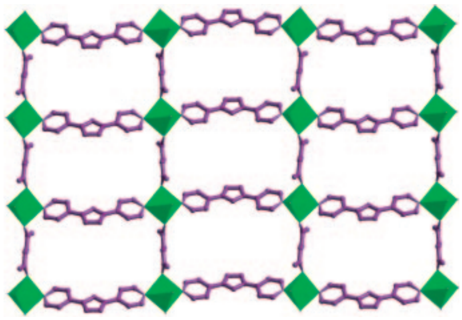

Figure 12. 2-D square grid coordination framework of $\{[Ni(4\text{-bpo})(H_2O)_2(suc)]\cdot 5H_2O\}_n$ bridged by 4-bpo and succinate linkers.

two terminal pyridyl groups, whereas in the structure of its mercury(II) azide complex $[Hg(4\text{-bpo})_2(N_3)_2]_n$,[24b] the 4-bpo ligands provide a new bidentate coordination mode via one pyridyl and one oxadiazole nitrogen donors, which link the octahedral Hg^{II} centers to result in a 2-D bilayer coordination framework.

2.2.4 3-D Coordination Framework: In this issue, the Cu^{II} ion is observed to readily construct multifarious 3-D coordination frameworks with 4-bpo (sometimes with the aid of auxiliary co-ligands, especially the counter anions), in which the effect of anion on the assembled process is significant. For example, the metal complexation of various copper(II) salts with 4-bpo in the presence of ClO_4^-/PF_6^-, N_3^-, and SO_4^{2-} anions leads to the formation of three types of distinct 3-D coordination polymers. Direct mixing of 4-bpo with copper perchlorate in the methanol/water medium gives the product of $\{[Cu(4\text{-bpo})_2(H_2O)_2](ClO_4)(OH)\cdot 2.5H_2O\}_n$.[5a] In this structure, the octahedral Cu^{II} centers are connected by the 4-bpo spacers to form 3-D diamond-like networks, which are significantly distorted and of twofold interpenetration due to the existence of a large cavity for each single net (Figure 13 top). Notably, although the 4-bpo bridging ligands coordinate to Cu^{II} in a square-planar arrangement, the bent backbone of 4-bpo allows such metal centers to actually serve as distorted tetrahedral nodes to constitute the final 3-D framework. Moreover, this complex represents the first divalent copper coordination polymer with twofold interpenetrating diamond structure. More recently, assembly of 4-bpo with copper perchlorate under different conditions also gives rise to another 3-D diamond-type coordination framework, which interestingly, is of threefold interpenetration (Figure 13 bottom). Significantly, this crystalline solid may undergo a temperature-driven reversible single-crystal-to-single-crystal structural transformation between the room temperature (293 K) and low temperature (150 K) phases with the general formula of $\{[Cu(4\text{-bpo})_2(H_2O)](ClO_4)_2\cdot x(\text{solvent})\}_n$.[25a]

On the other hand, treatment of $\{[Cu(4\text{-bpo})_2(H_2O)_2](ClO_4)(OH)\cdot 2.5H_2O\}_n$ in aqueous solution in the presence of excess $NaPF_6$ leads to the formation of well-shaped prismatic blue crystals of $\{[Cu(4\text{-bpo})_2(H_2O)_2](PF_6)_2\cdot 1.25H_2O\}_n$.[25b] The two structures are isomorphous due to the similar nature of the counter anions. Furthermore, with the same reactive procedure except that PF_6^- is replaced by N_3^- and SO_4^{2-}, respectively, two fascinating 3-D coordination polymers $\{[Cu(4\text{-bpo})(\mu\text{-}N_3)_2]\cdot 1.5H_2O\}_n$ and $\{[Cu(4\text{-bpo})(H_2O)(SO_4)]\cdot 2H_2O\}_n$ can also be properly isolated.[25b] In both structures, the 3-D networks are built up from the linkages of Cu–anion coordination layers via 4-bpo pillars, which however completely differ in the resultant network topology. In $\{[Cu(4\text{-bpo})(\mu\text{-}N_3)_2]\cdot 1.5H_2O\}_n$, the Cu^{II} centers are bridged by $\mu_{1,3}$-azide anions into (4,4) sheets (Figure 14 top), which are connected by the bridging 4-bpo ligands to afford a single acentric α-Po network with available channels (Figure 15 top). Whereas in the latter case, the sulfate anions are in μ_3-mode and bridge the Cu^{II} centers into (6,3) networks with alternating 3-connected Cu^{II} and sulfate nodes (Figure 14 bottom). The 2-D patterns are further extended by 4-bpo into a chiral channel-like 3-D framework (Figure 15 bottom) showing a (3,5)-connected network topology with the Schäfli symbol of $(6^3).(6^9.8)$.

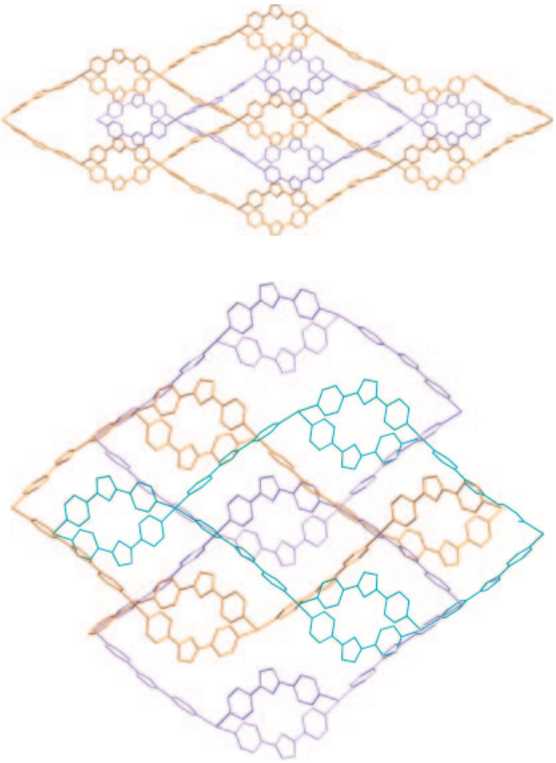

Figure 13. Schematic representation of (top) twofold and (bottom) threefold interpenetrated diamond coordination networks in two different 3-D copper(II) perchlorate complexes with 4-bpo.

And also, a 3-D microporous Cd^{II} coordination polymer $\{[Cd(4\text{-bpo})(SCN)_2]\cdot CH_3CN\}_n$ with 4-bpo and thiocyanate anionic bridges is presented,[25c] which is topologically equivalent to that of $\{[Cu(4\text{-bpo})(\mu\text{-}N_3)_2]\cdot 1.5H_2O\}_n$. In this case, the octahedral Cd^{II} centers are interlinked by the thiocyanate ions in $\mu_{N,S}$-fashion to form a 2-D sheet, featuring hourglass-shaped 16-membered $[Cd_4(\mu\text{-}SCN)_4]$ macrocycles as the repeating subunits (Figure 16 top). As shown in Figure 16 bottom, these 2-D layers are further linked by the bridging 4-bpo spacers to give a 3-D open framework with 1-D channels for the inclusion of lattice CH_3CN solvents.

2.3 Tridentate Coordination. Theoretically, besides the terminal pyridyl groups, the central oxadiazole entity may also

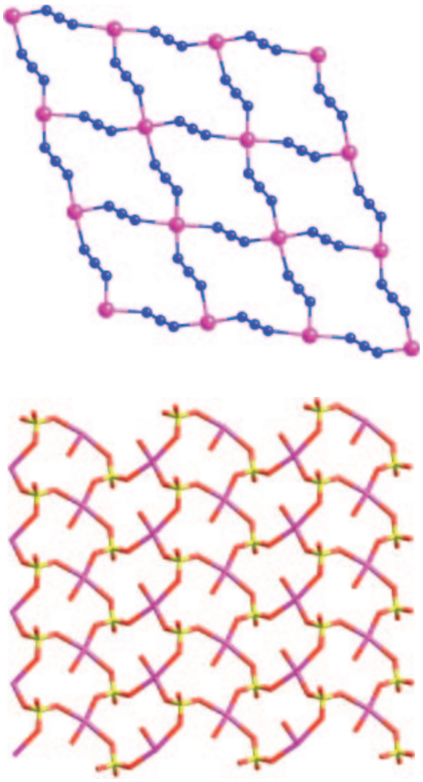

Figure 14. 2-D coordination layers of (top) Cu–azide in $\{[Cu(4\text{-bpo})(\mu\text{-}N_3)_2]\cdot1.5H_2O\}_n$ and (bottom) Cu–sulfate in $\{[Cu(4\text{-bpo})(H_2O)(SO_4)]\cdot2H_2O\}_n$.

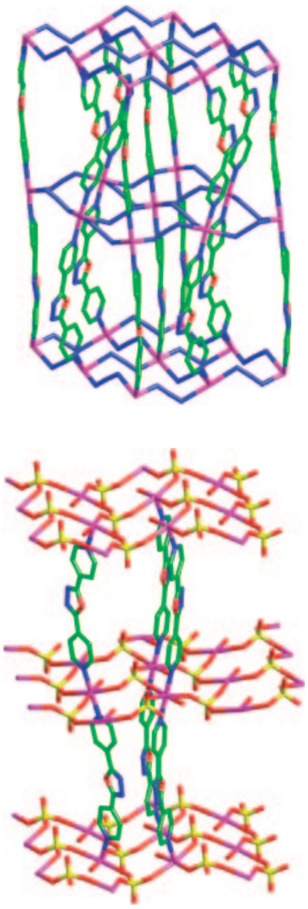

Figure 15. 3-D coordination frameworks of (top) $\{[Cu(4\text{-bpo})(\mu\text{-}N_3)_2]\cdot1.5H_2O\}_n$ and (bottom) $\{[Cu(4\text{-bpo})(H_2O)(SO_4)]\cdot2H_2O\}_n$.

be a potential candidate for metal complexation. However, as a matter of fact, it shows inert coordination tendency when encountering the common transition-metal ions. Nevertheless, it is worthwhile to point out that the coordination interaction between oxadiazole and the versatile Ag^I ion appears to be exercisable. Benefiting from the subtle templating effect of the counter anions and solvent molecules, the 4-bpo ligand may display flexible coordination styles in its polymeric Ag^I compounds. In this context, crystallization of 4-bpo with $AgSbF_6/AgPF_6$ in methanol/methylene chloride affords two isostructural 2-D coordination polymers $\{[Ag(4\text{-bpo})](SbF_6)\}_n$ and $\{[Ag(4\text{-bpo})](PF_6)\}_n$.[20b] In both structures, each Ag^I center adopts a distorted trigonal coordination environment and each 4-bpo ligand is bound to three Ag^I ions via one oxadiazole and two pyridyl nitrogen donors. Thus, the resultant cationic infinite polymeric network (Figure 17) consists of equal 3-connected nodes of Ag^I and 4-bpo, featuring a 4.8^2 network topology.

3. Influencing Factors on Structural Assembly

Generally speaking, the two basic elements for determining the structure and properties of a given supramolecular complex are organic ligand and metal ion. From the above discussion, it can be clearly revealed that the use of 3-bpo and 4-bpo building blocks with different orientations of the functional pyridyl groups as well as the selection of metal ions with dissimilar coordination tendency/geometry can result in significant structural diversity of the final crystalline materials (from discrete 0-D, to infinite 1-D, 2-D, and 3-D coordination architectures). On the other hand, it has been well known that some subtle but crucial influencing factors on coordination assemblies, such as the counter anion, solvent system, and even metal/ligand stoichiometric ratio, may also lead to the formation of distinct crystalline products. As expected, this is realized as the important terms to design and construct various metallosupramolecular systems on the basis of the 4-bpo and 3-bpo ligands as described below.

3.1 Anion Effect. In this direction, we have systematically investigated the anion effect on regulating the Cu^{II} coordination architectures with 3-bpo and 4-bpo. Explanatorily, the ancillary dicarboxylate components can be assessed as the organic anions thereof. In a typical procedure, all other parameters such as ligand, metal ion, solvent, and metal/ligand ratio are invariable with the only change of counter anion in the assembled process.[18a] With regard to 3-bpo, bimetallic macrocyclic coordination motifs are found in $[Cu_2(3\text{-bpo})_2(H_2O)_6](ClO_4)_4\cdot4H_2O$ and $[\{Cu(NO_3)_2(3\text{-bpo})\}_2]\cdot2CH_3CN$, in which the perchlorate moiety acts as the counter anion for charge balance and also forms hydrogen bonding with water, and the nitrate anions are bound to the Cu^{II} centers and involved in intermolecular C–H···O interactions to link the dinuclear units into 1-D arrays. As for the 1-D coordination polymers $\{[Cu_2(3\text{-bpo})_2(H_2O)_6(SO_4)_2]\cdot6H_2O\}_n$ and $\{[Cu_2(3\text{-bpo})(\mu\text{-}OAc)_4]\}_n$, the sulfate anions coordinate to the Cu^{II} centers in unidentate

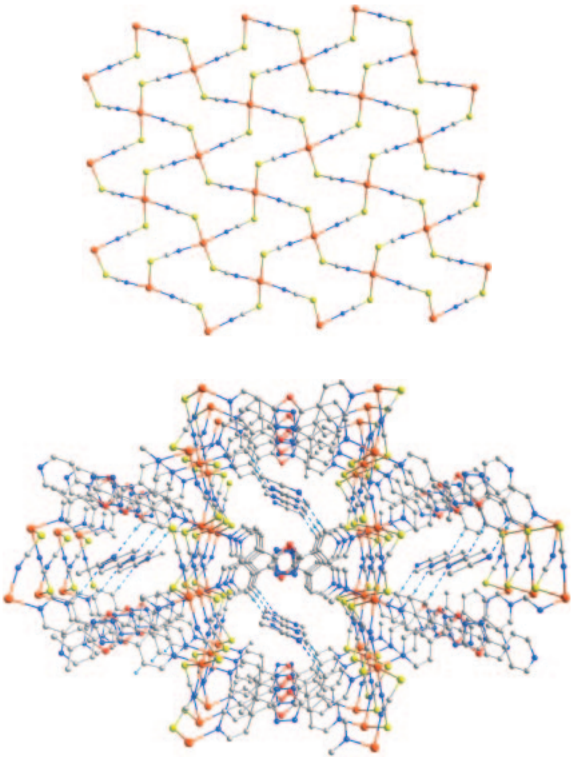

Figure 16. Views of $\{[Cd(4\text{-bpo})(SCN)_2]\cdot CH_3CN\}_n$. (top) 2-D Cd–thiocyanate coordination layer and (bottom) 3-D microporous network with the inclusion of solvents.

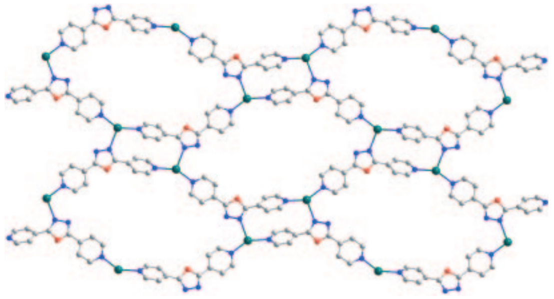

Figure 17. 2-D 4.8^2 polymeric cationic network bridged by tridentate 4-bpo ligands in the structures of $\{[Ag(4\text{-bpo})](SbF_6)\}_n$ and $\{[Ag(4\text{-bpo})](PF_6)\}_n$.

mode whereas the acetate components bridge the Cu^{II} ions in syn–syn fashion to define the $[Cu_2(\mu\text{-OAc})_4]$ subunit. Notably, in these structures, the different anions used in the assembled procedures can also extremely influence the conformation and arrangement of the 3-bpo ligands in the final crystalline products and thus afford distinct coordination arrays. With the employment of the organic anions of suc^{2-} and $Hfum^-$, two distinct complexes $\{[Cu(3\text{-bpo})(H_2O)_2(\mu\text{-suc})]\cdot 1.75H_2O\}_n$ and $[Cu(Hfum)_2(3\text{-bpo})(H_2O)]_2\cdot 2(3\text{-bpo})\cdot 6H_2O$ are obtained, and their 2-D layered and binuclear coordination patterns are constructed by *cisoid-I*-3-bpo spacers and anionic co-ligands of suc^{2-} bridges and $Hfum^-$ terminals, respectively.[18c]

In contrast to the 3-bpo related complexes, the well-defined coordination polymers derived from 4-bpo as well as various Cu^{II} salts experience a more significant structural diversity relying on the particular anions, including OAc^- (mononuclear),[5a] ClO_4^- (3-D),[5a] SO_4^{2-} (3-D),[25b] N_3^- (3-D),[25b] PF_6^- (3-D),[25b] and organic ions such as $pydc^{2-}$ (binuclear)[17c] and $chdc^{2-}$ (2-D).[24a] From the description above, it is especially interesting that the molecular structures of its Cu^{II} complexes are profoundly influenced by the anions with different coordination ability or bulk. In addition, the investigation of coordination chemistry of 4-bpo with Ag^I indicates the templating effect of counter ions on the resultant coordination architectures. In this regard, the existence and ancillary ligation of different anions, such as NO_3^-,[22d] BF_4^-,[16b] ClO_4^-,[22e] $CF_3SO_3^-$,[22e] PF_6^-,[20b] and SbF_6^-[20b] have been explored. For the first four species, the final structures are 1-D chain motifs, whereas corrugated 2-D layered frameworks are generated in the latter two cases. On the other hand, a greatly similar analog of 4-bpo, 2,5-bis(4-pyridyl)-1,3,4-thiadiazole (4-bpt) has been surveyed in the direction of silver coordination polymers with diverse anions such as PF_6^-, ClO_4^-, NO_3^-, and $CF_3SO_3^-$.[21a] The results reveal that the nature of anions is the underlying reason behind the structural difference of this series of Ag^I complexes. The PF_6^- and ClO_4^- anions have similar size and display poor coordination ability, and thereby in complexes $\{[Ag(4\text{-bpt})](PF_6)\}_n$ and $\{[Ag(4\text{-bpt})](ClO_4)\}_n$, the anionic components may play a spacial templating role in building up the 2-D coordination frameworks with cavities except for the essential charge balance. With regard to the supramolecular array of $\{[Ag_4(4\text{-bpt})_4(NO_3)_2](NO_3)_2\}_n$, the smaller NO_3^- anions possess stronger coordination or donor ability than those of PF_6^- and ClO_4^-, and serve as linkages to bridge the 1-D coordination chains to a 3-D framework via $Ag–O_{nitrate}$ contacts. As for another 1-D coordination polymer $\{[Ag(4\text{-bpt})](CF_3SO_3)\}_n$, the $CF_3SO_3^-$ ions with large bulk lie between the $\{[Ag(4\text{-bpt})]^+\}_n$ chains and prevent the further extension of these 1-D arrays, which may also act as the templates in structurally directing the overall 3-D lattice.

3.2 Solvent Effect. The self-assembly synthesis of specific reactants has been definitely affected by the reaction medium in thermodynamic and kinetic manners, which may produce different crystalline products from the mother solution under appropriate conditions. In this regard, a typical example is the delicate formation of two closely related coordination species $\{[Cu(4\text{-bpo})_2(H_2O)](ClO_4)_2\cdot x(\text{solvent})\}_n$[25a] and $\{[Cu(4\text{-bpo})_2(H_2O)_2](ClO_4)(OH)\cdot 2.5H_2O\}_n$,[5a] which are obtained from the same reagents but in different solvent medium ($CH_3OH/CHCl_3$ and CH_3OH/H_2O, respectively) and thus display dissimilar threefold and twofold interpenetrating coordination frameworks with the same diamond network topology.

3.3 Metal/Ligand Stoichiometric Ratio. The appropriate metal/ligand stoichiometric ratio applied during the synthetic procedure of a specific coordination supramolecular system can not only facilitate the crystallization process and/or regulate the competition of counterparts, but also diversify the molar ratio of the metal/ligand components in the final products and thus undoubtedly affect their crystal structures. It has been indicated that the M/4-bpo/thiocyanate ternary systems ($M = Co^{II}$, Mn^{II}, and Cd^{II}) possess the general formula $[M(bpo)_2(H_2O)_2(NCS)_2]$[17a,17b] and simple monomeric structures, in which both 4-bpo and thiocyanate anion only act as the unidendate terminal ligands. However, by varying the metal/ligand ratio in the assembled process of the Cd^{II} species, a novel 3-D open coordination framework $\{[Cd(4\text{-bpo})(SCN)_2]\cdot CH_3CN\}_n$[25c] can also be isolated as the pure phase, in which both 4-bpo and thiocyanate components serve as suitable connectors to result in the extended coordination architecture.

4. Physicochemical Properties of the Coordination Solids

4.1 Fluorescence. The rational design and preparation of inorganic–organic hybrid coordination solids, especially for those involving d^{10} metal ions and ligands with aromatic backbones have now been a powerful approach for achieving new luminescent materials. Owing to the ability of affecting the emission wavelength of organic ligand molecules, the deliberate construction of such crystalline species by the judicious choice of organic spacers and metal centers has been applied to obtain a variety of electroluminescent materials. In the solid state, the fluorescence spectra of 3-bpo and 4-bpo exhibit emission maxima at 360 and 358 nm, respectively.[20a,22c] As for the relevant polymeric metal complexes with the 3-bpo ligand, the emission spectrum of $[Hg(3\text{-bpo})I_2]_n$ is red-shifted to 427 nm, whereas for $[Zn(3\text{-bpo})Cl_2]_n$, the emission maximum is blue-shifted to 329 nm.[22c] That is to say, the emission of 3-bpo may be significantly affected and tuned by the incorporation of Zn^{II} or Hg^{II} metal ions, which may be assigned to the ligand-to-metal charge transfer (LMCT) in these coordination polymers. On the other hand, the emissions of $[Zn(3\text{-bpo})(H_2O)_3(NO_3)]_2(NO_3)_2$ and $[\{Cu(NO_3)_2(3\text{-bpo})\}_2]\cdot 2CH_3CN$ in the solid state are both red-shifted to 367 and 380 nm, rspectively.[20a] Reasonably, the presence of intervening Zn^{II} and Cu^{II} ions, which exert an electron-withdrawing effect as a consequence of their bivalent charge and the attached nitrate ion, has a significant influence on the fluorescent properties of the resultant coordination complexes.

Similarly, the red-shifted phenomenon can be also discovered in the 4-bpo related coordination polymers. For instance,[25a] $\{[Cu(4\text{-bpo})_2(H_2O)](ClO_4)_2\}_n$ is luminescent in the solid state, and exhibits one fluorescence emission maximum at 373 nm (358 nm for the free 4-bpo ligand) upon photoexcitation at 213 nm, which should originate from the ligand-centered n–π^* or π–π^* process.

4.2 Anion Exchange. Normally, the nature of anion plays a key role in the formation of these coordination frameworks, especially for the Cu^{II} species according to the above description. Consequently, the anion-exchange behaviors of the Cu^{II}-related coordination complexes are deliberately taken into consideration. For example,[25b] compound $\{[Cu(4\text{-bpo})_2(H_2O)_2](PF_6)_2\cdot 1.25H_2O\}_n$ can be obtained by reacting $\{[Cu(4\text{-bpo})_2(H_2O)_2](ClO_4)(OH)\cdot 2.5H_2O\}_n$ with excess $NaPF_6$ in aqueous solution, and this procedure is reversible. Moreover, two novel acentric or chiral 3-D coordination polymers $\{[Cu(4\text{-bpo})(\mu\text{-}N_3)_2]\cdot 1.5H_2O\}_n$ and $\{[Cu(4\text{-bpo})(H_2O)(SO_4)]\cdot 2H_2O\}_n$ can also be achieved either from $\{[Cu(4\text{-bpo})_2(H_2O)_2](ClO_4)(OH)\cdot 2.5H_2O\}_n$ or $\{[Cu(4\text{-bpo})_2(H_2O)_2](PF_6)_2\cdot 1.25H_2O\}_n$ in the presence of NaN_3 or Na_2SO_4 through the anion-exchange procedure. It seems that the exchange reaction occurs via dissolution of the precursor before (or simultaneously with) crystallization of the final product in these courses.

In addition, selective anion-exchange function of a series of PtS-type metal–organic frameworks based on various silver(I) salts and an analogous ligand 2,5-bis(pyrazine)-1,3,4-oxadiazole has also been demonstrated.[26] Notably, in this case, the host coordination frameworks are almost invariable although the anions vary significantly from the smaller BF_4^-, AsF_6^-, and $CF_3SO_3^-$ to the very large SbF_6^- with different binding abilities to silver(I), and the mechanism of anion exchange seems to be a solvent-mediated process.

4.3 Magnetism. The coordination architectures presented herein are usually based on the isolated metal ions that are connected through 3-bpo/4-bpo ditopic organic ligands and/or additional assistant linkers. Under such conditions, the magnetic coupling via 3-bpo and 4-bpo bridges mainly depends on the distance between the metal ions. As a matter of fact, the 3-bpo and 4-bpo ligands cannot mediate the magnetic interactions effectively because the possible overlap of magnetic orbitals through such long organic bridges is negligible. Thus, it can be anticipated that such ligands do not essentially contribute to the magnetic properties in their complexes and the resultant magnetic systems will be paramagnetic only (very small intra- or intermolecular exchange interactions may occur at very low temperature).[5a,6a,18a,18c,25b] Nevertheless, some interesting magnetic phenomena have been observed due to the linkage of metal ions via other small anionic bridges in these complexes. For instance,[25b] the 3-D coordination polymer $\{[Cu(4\text{-bpo})(\mu\text{-}N_3)_2]\cdot 1.5H_2O\}_n$ contains unique 2-D Cu–N_3 layers with a new topological type that are pillared by the 4-bpo linkers. Small antiferromagnetic interactions are found between the adjacent Cu^{II} ions via the azide anions in end-to-end coordination mode. While in another 3-D complex $\{[Cu(4\text{-bpo})(H_2O)(SO_4)]\cdot 2H_2O\}_n$, unexpected weak ferromagnetic coupling between the Cu^{II} ions are observed for the first time within the 2-D Cu–sulfate coordination layers. At present, we may only briefly conclude that the bent geometric features of 3-bpo and 4-bpo will influence and modulate the metal–anion inorganic magnetic arrays in the resultant ternary coordination systems. Based on this strategy, more interesting magnetic materials may be obtained by using other anionic bridges that can effectively transfer the magnetic interactions between the paramagnetic metal ions, with the aid of the 3-bpo and 4-bpo components that can lead to the formation of novel coordination networks.

4.4 Guest Inclusion. Ordinarily, the known 3-D coordination frameworks of 4-bpo and related ligand 4-bpt (vide ante) possess considerable channels for the inclusion of different guests and/or anions. However, these microporous materials show completely different guest absorption/desorption behaviors. First, the crystalline samples of 3-D coordination polymers $\{[Cu(4\text{-bpo})_2(H_2O)_2](ClO_4)(OH)\cdot 2.5H_2O\}_n$ and $\{[Cu(4\text{-bpo})_2(H_2O)_2](PF_6)_2\cdot 1.25H_2O\}_n$ are not stable when exposed to air at room temperature, and partly change to the amorphous substance.[5a,25b] This is usually observed for coordination polymers with large cavities. Second, as for the 3-D metal–organic frameworks $\{[Cd(4\text{-bpo})(SCN)_2]\cdot CH_3CN\}_n$, $\{[Cu(4\text{-bpo})(H_2O)(SO_4)]\cdot 2H_2O\}_n$, and its isostructural complex $\{[Cu(4\text{-bpt})(H_2O)(SO_4)](H_2O)_2\}_n$, the guest solvent molecules can be successfully removed from the crystalline lattices to result in microporous materials, whose structures correspondingly coincide with those of the original coordination polymers. Moreover, the included solvent molecules can be easily reintroduced into the evacuated samples without change of the crystal structures.[6a,25b,25c] While finally, coordination polymer $\{[Cd(4\text{-bpt})(NCS)_2]\cdot 1.5CH_3OH\}_n$ has a similar 3-D network (not isostructural) to that of $\{[Cd(4\text{-bpo})(SCN)_2]\cdot CH_3CN\}_n$, but represents another type of microporous framework which has dissimilar guest inclusion behavior. In this case, the removal of guest molecules makes a structural change of the network solid, which however, can revert to the original structure by reintroducing the guest molecules.[6a]

In this context, it seems that the counter anions are not only critical to the network architectures of coordination solids but also to their possible functions. Generally speaking, for the known 3-D metal–organic frameworks based on 3-bpo and 4-bpo, the bulk counter anions with poor coordination ability always occupy the empty cavity and serve for guests to template the coordination architectures, which may be exchanged or replaced by other ions to afford new crystalline species. Of further interest, small counter anions especially halogens and pseudo-halogens with strong and versatile binding features may lead to the generation of neutral coordination frameworks with included solvent molecules, which can be easily removed from the crystalline lattices to afford microporous crystalline materials with attractive functions. On the other hand, such coordination systems with the paramagnetic metal ions may also show interesting magnetic properties. Moreover, organic polycarboxylate anions have also been confirmed to be effective co-ligands to design and construct unusual coordination frameworks, which may possess available channels and thus potential porosity. However, the related systems involving 3-bpo and 4-bpo have largely been unexplored, and we are currently extending this strategy to prepare new coordination polymers.

5. Conclusion and Outlook

A pair of analogous angular dipyridyl ligands 2,5-bis(*n*-pyridyl)-1,3,4-oxadiazole ($n = 3$ for 3-bpo and $n = 4$ for 4-bpo) have been applied as versatile prototypical building blocks to construct a variety of coordination supramolecular systems, and the network architectures are argued to heavily depend on the coordination mode and/or conformation of such ligands when coordinating to different metal ions. A variety of coordination fashions featured in the known complexes are enumerated in order of the ligation number to the metal ions, including monodentate, bidentate, and tridentate modes, as well as the occurrence of different cisoid-I, cisoid-II, and transoid conformations for 3-bpo. In a normal manner, the variation in number and orientation of the ligated donors is predominantly responsible for the formation of different polymeric coordination arrays. Consequently, the resultant architectures can present discrete mononuclear entities and binuclear motifs of metallamacrocycle or cage, as well as infinite 1-D zigzag, double sinusoidal, comb-like, or binuclear paddle-wheel based chains, 2-D layered networks, and 3-D open and interpenetrated frameworks, which may display some useful properties such as fluorescence, magnetism, anion exchange, and guest inclusion relying on their crystalline structures. Beyond this, concerning the sound role of ancillary stimulation during the assembled process, other subtle factors such as counter anion, solvent system, and metal/ligand stoichiometric ratio have also been found to be crucial to regulate the construction of metallosupramolecular architectures.

At this stage, such angular ligands with the oxadiazole-spacer are generally considered to be elongated analogs of dipyridyl, and of further importance, the modification of these building blocks can be easily achieved by employing other functional groups to replace the terminal pyridyl rings,[26] profiting from the sophisticated ligand design strategy. Therefore, it can be optimistically predicted that more coordination crystalline materials with these modified ligands will be exploited for their novel structural features and potential applications as functional hybrid materials.

We thank all present and former co-workers who are involved in the different research projects. We are grateful for the financial support from the 973 Program of China, NSFC, and NSF of Tianjin, China.

References

1 For examples: a) M. J. Zaworotko, *Chem. Commun.* **2001**, 1. b) G. R. Desiraju, *Angew. Chem., Int. Ed.* **2007**, *46*, 8342. c) M. W. Hosseini, *Acc. Chem. Res.* **2005**, *38*, 313. d) G. M. J. Schmidt, *Pure Appl. Chem.* **1971**, *27*, 647. e) S. Kitagawa, R. Kitaura, S. Noro, *Angew. Chem., Int. Ed.* **2004**, *43*, 2334. f) J.-M. Lehn, *Supramolecular Chemistry*, VCH, Weinheim, Germany, **1995**. g) P. Comba, W. Schiek, *Coord. Chem. Rev.* **2003**, *238–239*, 21. h) J. D. Badjić, A. Nelson, S. J. Cantrill, W. B. Turnbull, J. F. Stoddart, *Acc. Chem. Res.* **2005**, *38*, 723.

2 For examples: a) S. J. Lee, W. Lin, *Acc. Chem. Res.* **2008**, *41*, 521. b) P. D. Beer, P. A. Gale, *Angew. Chem., Int. Ed.* **2001**, *40*, 486. c) F. P. Schmidtchen, M. Berger, *Chem. Rev.* **1997**, *97*, 1609. d) E. Coronado, J. R. Galán-Mascarós, C. J. Gomez-Garcia, V. Laukhin, *Nature* **2000**, *408*, 447. e) O. Kahn, *Acc. Chem. Res.* **2000**, *33*, 647. f) B. Moulton, J. Lu, R. Hajndl, S. Hariharan, M. J. Zaworotko, *Angew. Chem., Int. Ed.* **2002**, *41*, 2821. g) M. Kondo, M. Shimamura, S. Noro, S. Minakoshi, A. Asami, K. Seki, S. Kitagawa, *Chem. Mater.* **2000**, *12*, 1288. h) J. S. Seo, D. Whang, H. Lee, S. I. Jun, J. Oh, Y. J. Jeon, K. Kim, *Nature* **2000**, *404*, 982. i) M. Fujita, Y. J. Kwon, S. Washizu, K. Ogura, *J. Am. Chem. Soc.* **1994**, *116*, 1151. j) M. Sasa, K. Tanaka, X.-H. Bu, M. Shiro, M. Shionoya, *J. Am. Chem. Soc.* **2001**, *123*, 10750. k) J.-R. Li, Q. Yu, E. C. Sañudo, Y. Tao, W.-C. Song, X.-H. Bu, *Chem. Mater.* **2008**, *20*, 1218. l) Y.-F. Zeng, X. Hu, F.-C. Liu, X.-H. Bu, *Chem. Soc. Rev.* **2009**, *38*, 469.

3 a) M. D. Ward, *Chem. Commun.* **2005**, 5838. b) L. Brammer, *Chem. Soc. Rev.* **2004**, *33*, 476. c) C. Janiak, *Dalton Trans.* **2003**, 2781. d) D. Braga, *Chem. Commun.* **2003**, 2751. e) A. Y. Robin, K. M. Fromm, *Coord. Chem. Rev.* **2006**, *250*, 2127.

4 a) A. F. Wells, *Three-dimensional Nets and Polyhedra*, Wiley, New York, **1977**. b) A. J. Blake, N. R. Champness, P. Hubberstey, W.-S. Li, M. A. Withersby, M. Schröder, *Coord. Chem. Rev.* **1999**, *183*, 117. c) S. A. Barnett, N. R. Champness, *Coord. Chem. Rev.* **2003**, *246*, 145. d) M. Du, C.-P. Li, X.-J. Zhao, *Cryst. Growth Des.* **2006**, *6*, 335. e) S.-L. Zheng, M.-L. Tong, X.-M. Chen, *Coord. Chem. Rev.* **2003**, *246*, 185. f) A. F. Wells, *Structural Inorganic Chemistry*, 5th ed., Oxford University Press, Oxford, **1984**.

5 a) M. Du, X.-H. Bu, Y.-M. Guo, H. Liu, S. R. Batten, J. Ribas, T. C. W. Mak, *Inorg. Chem.* **2002**, *41*, 4904. b) T. J. Prior, M. J. Rosseinsky, *Chem. Commun.* **2001**, 495. c) X.-M. Zhang,

R.-Q. Fang, H.-S. Wu, *J. Am. Chem. Soc.* **2005**, *127*, 7670. d) X.-H. Bu, K. Tanaka, M. Shionoya, K. Biradha, H. Morishita, S. Furusho, *Chem. Commun.* **2000**, 971.

6 a) Z. Huang, H.-B. Song, M. Du, S.-T. Chen, X.-H. Bu, J. Ribas, *Inorg. Chem.* **2004**, *43*, 931. b) K. Biradha, M. Sarkar, L. Rajput, *Chem. Commun.* **2006**, 4169. c) K. Biradha, M. Fujita, *Chem. Commun.* **2001**, 15. d) H. Hou, L. Xie, G. Li, T. Ge, Y. Fan, Y. Zhu, *New J. Chem.* **2004**, *28*, 191. e) B.-H. Ye, M.-L. Tong, X.-M. Chen, *Coord. Chem. Rev.* **2005**, *249*, 545. f) O. R. Evans, H. L. Ngo, W. Lin, *J. Am. Chem. Soc.* **2001**, *123*, 10395.

7 For examples: a) X.-H. Bu, W. Chen, S.-L. Lu, R.-H. Zhang, D.-Z. Liao, W.-M. Bu, M. Shionoya, F. Brisse, J. Ribas, *Angew. Chem., Int. Ed.* **2001**, *40*, 3201. b) X.-H. Bu, W. Chen, M. Du, R.-H. Zhang, *CrystEngComm* **2001**, *3*, 131. c) X.-H. Bu, W. Weng, M. Du, W. Chen, J.-R. Li, R.-H. Zhang, L.-J. Zhao, *Inorg. Chem.* **2002**, *41*, 1007. d) X.-H. Bu, W. Weng, J.-R. Li, W. Chen, R.-H. Zhang, *Inorg. Chem.* **2002**, *41*, 413. e) J.-R. Li, X.-H. Bu, R.-H. Zhang, *Inorg. Chem.* **2004**, *43*, 237. f) J.-R. Li, R.-H. Zhang, X.-H. Bu, *Cryst. Growth Des.* **2004**, *4*, 219. g) J.-R. Li, X.-H. Bu, R.-H. Zhang, *Dalton Trans.* **2004**, 813. h) J.-R. Li, X.-H. Bu, R.-H. Zhang, J. Ribas, *Cryst. Growth Des.* **2005**, *5*, 1919. i) J.-R. Li, W.-T. Chen, M.-L. Tong, G.-C. Guo, Y. Tao, Q. Yu, W.-C. Song, X.-H. Bu, *Cryst. Growth Des.* **2008**, *8*, 2780.

8 For examples: a) X.-H. Bu, W. Chen, M. Du, K. Biradha, W.-Z. Wang, R.-H. Zhang, *Inorg. Chem.* **2002**, *41*, 437. b) X.-H. Bu, W. Chen, W.-F. Hou, M. Du, R.-H. Zhang, F. Brisse, *Inorg. Chem.* **2002**, *41*, 3477. c) J.-R. Li, X.-H. Bu, J. Jiao, W.-P. Du, X.-H. Xu, R.-H. Zhang, *Dalton Trans.* **2005**, 464. d) Y. Zheng, M. Du, J.-R. Li, R.-H. Zhang, X.-H. Bu, *Dalton Trans.* **2003**, 1509. e) R.-F. Song, Y.-B. Xie, J.-R. Li, X.-H. Bu, *Dalton Trans.* **2003**, 4742. f) J.-R. Li, R.-H. Zhang, X.-H. Bu, *Cryst. Growth Des.* **2003**, *3*, 829. g) Y. Zheng, J.-R. Li, M. Du, R.-Q. Zou, X.-H. Bu, *Cryst. Growth Des.* **2005**, *5*, 215. h) X.-H. Bu, W.-F. Hou, M. Du, W. Chen, R.-H. Zhang, *Cryst. Growth Des.* **2002**, *2*, 303.

9 For examples: a) M. Du, X.-H. Bu, Y.-M. Guo, J. Ribas, *Chem.—Eur. J.* **2004**, *10*, 1345. b) M. Du, X.-H. Bu, Y.-M. Guo, L. Zhang, D.-Z. Liao, J. Ribas, *Chem. Commun.* **2002**, 1478. c) M. Du, X.-H. Bu, Y.-M. Guo, J. Ribas, C. Diaz, *Chem. Commun.* **2002**, 2550. d) X.-H. Bu, M. Du, Z.-L. Shang, R.-H. Zhang, D.-Z. Liao, M. Shionoya, T. Clifford, *Inorg. Chem.* **2000**, *39*, 4190. e) X.-H. Bu, M. Du, L. Zhang, Z.-L. Shang, R.-H. Zhang, M. Shionoya, *J. Chem. Soc., Dalton Trans.* **2001**, 729. f) X.-H. Bu, M. Du, L. Zhang, Z.-L. Shang, R.-H. Zhang, *J. Chem. Soc., Dalton Trans.* **2001**, 593.

10 For examples: a) X.-H. Bu, K. Tanaka, M. Shionoya, K. Biradha, T. Yamaguchi, M. Nishimura, T. Ito, *Chem. Commun.* **2000**, 1953. b) T.-L. Hu, J.-R. Li, C.-S. Liu, X.-S. Shi, J.-N. Zhou, X.-H. Bu, J. Ribas, *Inorg. Chem.* **2006**, *45*, 162. c) R.-Q. Zou, X.-H. Bu, R.-H. Zhang, *Inorg. Chem.* **2004**, *43*, 5382. d) X.-H. Bu, H. Liu, M. Du, L. Zhang, Y.-M. Guo, M. Shionoya, J. Ribas, *Inorg. Chem.* **2002**, *41*, 1855. e) X.-H. Bu, H. Liu, M. Du, K. M.-C. Wong, V. W.-W. Yam, M. Shionoya, *Inorg. Chem.* **2001**, *40*, 4143. f) J.-R. Li, Y. Tao, Q. Yu, X.-H. Bu, H. Sakamoto, S. Kitagawa, *Chem.—Eur. J.* **2008**, *14*, 2771.

11 For examples: a) X.-H. Bu, M.-L. Tong, H.-C. Chang, S. Kitagawa, S. R. Batten, *Angew. Chem., Int. Ed.* **2004**, *43*, 192. b) J.-R. Li, Y. Tao, Q. Yu, X.-H. Bu, *Chem. Commun.* **2007**, 1527. c) C.-S. Liu, J.-J. Wang, L.-F. Yan, Z. Chang, X.-H. Bu, E. C. Sañudo, J. Ribas, *Inorg. Chem.* **2007**, *46*, 6299. d) C.-S. Liu, P.-Q. Chen, E.-C. Yang, J.-L. Tian, X.-H. Bu, Z.-M. Li, H.-W. Sun, Z. Lin, *Inorg. Chem.* **2006**, *45*, 5812. e) T.-L. Hu, J.-R. Li, Y.-B. Xie, X.-H. Bu, *Cryst. Growth Des.* **2006**, *6*, 648.

12 For examples: a) Y.-F. Zeng, J.-P. Zhao, B.-W. Hu, X. Hu, F.-C. Liu, J. Ribas, J. Ribas-Ariño, X.-H. Bu, *Chem.—Eur. J.* **2007**, *13*, 9924. b) J.-R. Li, Q. Yu, Y. Tao, X.-H. Bu, J. Ribas, S. R. Batten, *Chem. Commun.* **2007**, 2290. c) J.-R. Li, Q. Yu, E. C. Sañudo, Y. Tao, X.-H. Bu, *Chem. Commun.* **2007**, 2602. d) Y.-F. Zeng, F.-C. Liu, J.-P. Zhao, S. Cai, X.-H. Bu, J. Ribas, *Chem. Commun.* **2006**, 2227. e) F.-C. Liu, Y.-F. Zeng, J.-P. Zhao, B.-W. Hu, X.-H. Bu, J. Ribas, J. Cano, *Inorg. Chem.* **2007**, *46*, 1520. f) Y.-F. Zeng, X. Hu, J.-P. Zhao, B.-W. Hu, E. C. Sañudo, F.-C. Liu, X.-H. Bu, *Chem.—Eur. J.* **2008**, *14*, 7127.

13 a) N. G. Pschirer, D. M. Ciurtin, M. D. Smith, U. H. F. Bunz, H.-C. zur Loye, *Angew. Chem., Int. Ed.* **2002**, *41*, 583. b) H. W. Roesky, M. Andruh, *Coord. Chem. Rev.* **2003**, *236*, 91.

14 a) J.-Y. Cheng, Y.-B. Dong, J.-P. Ma, R.-Q. Huang, M. D. Smith, *Inorg. Chem. Commun.* **2005**, *8*, 6. b) J.-Q. Wang, C.-X. Ren, G.-X. Jin, *Eur. J. Inorg. Chem.* **2006**, 3274. c) S. Liu, J. Zhang, X. Wang, G.-X. Jin, *Dalton Trans.* **2006**, 5225. d) M. Du, Z.-H. Zhang, X.-J. Zhao, *Cryst. Growth Des.* **2005**, *5*, 1199. e) M. Du, Z.-H. Zhang, X.-J. Zhao, *Cryst. Growth Des.* **2006**, *6*, 390.

15 a) M. Du, X.-J. Jiang, X.-J. Zhao, *Acta Crystallogr., Sect. E* **2005**, *61*, m485. b) X.-J. Zhao, J.-H. Guo, M. Du, *Acta Crystallogr., Sect. E* **2005**, *61*, m913.

16 a) M. Du, C.-P. Li, Y.-P. You, X.-J. Jiang, H. Cai, Q. Wang, J.-H. Guo, *Inorg. Chim. Acta* **2007**, *360*, 2169. b) M. Du, X.-J. Zhao, *J. Mol. Struct.* **2004**, *694*, 235. c) Y.-B. Dong, J.-P. Ma, R.-Q. Huang, F.-Z. Liang, M. D. Smith, *Dalton Trans.* **2003**, 1472.

17 a) Y.-Y. Fang, H. Liu, M. Du, Y.-M. Guo, X.-H. Bu, *J. Mol. Struct.* **2002**, *608*, 229. b) M. Du, H. Liu, X.-H. Bu, *J. Chem. Crystallogr.* **2002**, *32*, 57. c) M. Du, H. Cai, X.-J. Zhao, *Inorg. Chim. Acta* **2006**, *359*, 673.

18 a) M. Du, X.-H. Bu, Z. Huang, S.-T. Chen, Y.-M. Guo, C. Diaz, J. Ribas, *Inorg. Chem.* **2003**, *42*, 552. b) M. Du, X.-J. Zhao, J.-H. Guo, *Inorg. Chem. Commun.* **2005**, *8*, 1. c) M. Du, X.-J. Jiang, X.-J. Zhao, H. Cai, J. Ribas, *Eur. J. Inorg. Chem.* **2006**, 1245.

19 a) M. Du, Y.-M. Guo, X.-S. Shi, X.-H. Bu, J. Ribas, *Chin. J. Inorg. Chem.* **2004**, *20*, 1150. b) M. Du, Y.-M. Guo, X.-H. Bu, J. Ribas, M. Monfort, *New J. Chem.* **2002**, *26*, 645.

20 a) Y.-B. Dong, J.-Y. Cheng, H.-Y. Wang, R.-Q. Huang, B. Tang, M. D. Smith, H.-C. zur Loye, *Chem. Mater.* **2003**, *15*, 2593. b) Y.-B. Dong, J.-Y. Cheng, R.-Q. Huang, M. D. Smith, H.-C. zur Loye, *Inorg. Chem.* **2003**, *42*, 5699. c) J. Li, J.-P. Ma, J.-B. Xia, R.-Q. Huang, Y.-B. Dong, *Acta Crystallogr., Sect. E* **2006**, *62*, m247.

21 a) Z. Huang, M. Du, H.-B. Song, X.-H. Bu, *Cryst. Growth Des.* **2004**, *4*, 71. b) Y.-B. Dong, J.-P. Ma, M. D. Smith, R.-Q. Huang, B. Tang, D.-S. Guo, J.-S. Wang, H.-C. zur Loye, *Solid State Sci.* **2003**, *5*, 601.

22 a) M. Du, X.-J. Zhao, *J. Mol. Struct.* **2003**, *655*, 191. b) J.-Y. Cheng, Y.-B. Dong, R.-Q. Huang, M. D. Smith, *Inorg. Chim. Acta* **2005**, *358*, 891. c) Y.-B. Dong, J.-Y. Cheng, J.-P. Ma, H.-Y. Wang, R.-Q. Huang, D.-S. Guo, M. D. Smith, *Solid State Sci.* **2003**, *5*, 1177. d) Y.-M. Guo, H. Liu, X.-B. Leng, *Acta Crystallogr., Sect. E* **2003**, *59*, m59. e) Y.-B. Dong, J.-P. Ma, R.-Q. Huang, M. D. Smith, H.-C. zur Loye, *Inorg. Chem.* **2003**, *42*, 294. f) M. Du, C.-K. Lam, X.-H. Bu, T. C. W. Mak, *Inorg. Chem. Commun.* **2004**, *7*, 315.

23 a) Y.-B. Dong, J.-P. Ma, M. D. Smith, R.-Q. Huang, B. Tang, D. Chen, H.-C. zur Loye, *Solid State Sci.* **2002**, *4*, 1313. b) H. Liu, B.-H. Zhong, L.-P. Liu, S.-T. Han, *J. Chem. Crystallogr.* **2004**, *34*, 259.

24 a) M. Du, H. Cai, X.-J. Zhao, *Inorg. Chim. Acta* **2005**, *358*,

4034. b) N. Atoub, G. Mahmoudi, A. Morsali, *Inorg. Chem. Commun.* **2007**, *10*, 166.

25 a) J.-P. Ma, Y.-B. Dong, R.-Q. Huang, M. D. Smith, C.-Y. Su, *Inorg. Chem.* **2005**, *44*, 6143. b) M. Du, Y.-M. Guo, S.-T. Chen, X.-H. Bu, S. R. Batten, J. Ribas, S. Kitagawa, *Inorg. Chem.* **2004**, *43*, 1287. c) M. Du, S.-T. Chen, X.-H. Bu, *Cryst. Growth Des.* **2002**, *2*, 625.

26 M. Du, X.-J. Zhao, J.-H. Guo, S. R. Batten, *Chem. Commun.* **2005**, 4836.

Miao Du was born in China (1976). He received his B.S. from Nankai University (1998), and subsequently his doctorate there (2003) under the supervision of Prof. Xian-He Bu. Then, he joined the faculty at Tianjin Normal University and now is a Professor of Chemistry. He has worked with Prof. Thomas C. W. Mak at the Chinese University of Hong Kong and Dr. Qiang Xu at National Institute of Advanced Industrial Science and Technology of Japan (JSPS fellow). His current research lies in coordination chemistry and crystal engineering.

Xian-He Bu was born in 1964 in China. He studied in Nankai University and received his bachelor and doctorate in 1986 and 1992 under the direction of Prof. Yun-Ti Chen. He received another Ph.D. in pharmaceutical science at Hiroshima University in 1995 under the supervision of Prof. Eiichi Kimura. He has worked at IMS and the University of Tokyo with Prof. M. Shionoya, also at Kyoto University with Prof. S. Kitagawa as visiting scientist. He is now a full professor (Chang-Jiang Scholar) at Nankai University and serves as the head of the Department of Chemistry and a director of Tianjin Key Lab on Metal and Molecule-based Materials Chemistry. His current research interests include coordination chemistry, crystal engineering, MOFs, magnetic materials, etc.